Localized Waves

Edited by

HUGO E. HERNÁNDEZ-FIGUEROA
MICHEL ZAMBONI-RACHED
ERASMO RECAMI

THE WILEY BICENTENNIAL—KNOWLEDGE FOR GENERATIONS

*E*ach generation has its unique needs and aspirations. When Charles Wiley first opened his small printing shop in lower Manhattan in 1807, it was a generation of boundless potential searching for an identity. And we were there, helping to define a new American literary tradition. Over half a century later, in the midst of the Second Industrial Revolution, it was a generation focused on building the future. Once again, we were there, supplying the critical scientific, technical, and engineering knowledge that helped frame the world. Throughout the 20th Century, and into the new millennium, nations began to reach out beyond their own borders and a new international community was born. Wiley was there, expanding its operations around the world to enable a global exchange of ideas, opinions, and know-how.

For 200 years, Wiley has been an integral part of each generation's journey, enabling the flow of information and understanding necessary to meet their needs and fulfill their aspirations. Today, bold new technologies are changing the way we live and learn. Wiley will be there, providing you the must-have knowledge you need to imagine new worlds, new possibilities, and new opportunities.

Generations come and go, but you can always count on Wiley to provide you the knowledge you need, when and where you need it!

WILLIAM J. PESCE
PRESIDENT AND CHIEF EXECUTIVE OFFICER

PETER BOOTH WILEY
CHAIRMAN OF THE BOARD

Localized Waves

Edited by

HUGO E. HERNÁNDEZ-FIGUEROA
MICHEL ZAMBONI-RACHED
ERASMO RECAMI

◆ **IEEE**

IEEE PRESS

BICENTENNIAL
1807
⊛WILEY
2007
BICENTENNIAL

WILEY-
INTERSCIENCE

A JOHN WILEY & SONS, INC., PUBLICATION

Contents

Contributors

Ioannis M. Besieris, The Bradley Department of Electrical and Computer Engineering, Virginia Polytechnic Institute and State University, Blacksburg, Virginia

Martin Bock, Max-Born-Institute for Nonlinear Optics and Short-Pulse Spectroscopy, Berlin, Germany

Zdeněk Bouchal, Department of Optics, Palacký University, Olomouc, Czech Republic

Radek Čelechovský, Department of Optics, Palacký University, Olomouc, Czech Republic

Claudio Conti, Research Center Enrico Fermi, Rome, Italy, and Research Center SOFT INFM-CNR, University La Sapienza, Rome, Italy

Paolo Di Trapani, Dipartimento di Fisica e Matematica, Università degli Studi dell'Insubria sede di Como, Como, Italy

Ari T. Friberg, Department of Microelectronics and Applied Physics, Royal Institute of Technology, Kista, Sweden

Uwe Griebner, Max-Born-Institute for Nonlinear Optics and Short-Pulse Spectroscopy, Berlin, Germany

Ruediger Grunwald, Max-Born-Institute for Nonlinear Optics and Short-Pulse Spectroscopy, Berlin, Germany

Hugo E. Hernández-Figueroa, Faculdade de Engenharia Elétrica e de Computação, Departamento de Microonda e Óptica, Universidade Estadual de Campinas, Campinas, SP, Brazil

Wei Hu, Laboratory of Photonic Information Technology, School for Information and Optoelectronic Science and Technology, South China Normal University, Guangzhou, P. R. China

Davide Janner, Dipartimento di Fisica, Politecnico di Milano, Milan, Italy

Volker Kebbel, Automation and Assembly Technologies GmbH, Bremen, Germany

Sergei V. Kukhlevsky, Department of Experimental Physics, Institute of Physics, University of Pécs, Pécs, Hungary

Stefano Longhi, Dipartimento di Fisica, Politecnico di Milano, Milan, Italy

Jian-yu Lu, Ultrasound Laboratory, Department of Bioengineering, The University of Toledo, Toledo, Ohio

Iacopo Mochi, Nello Carrara Institute of Applied Physics–CNR, Florence Research Area, Sesto Fiorentino, Italy

Daniela Mugnai, Nello Carrara Institute of Applied Physics–CNR, Florence Research Area, Sesto Fiorentino, Italy

Uwe Neumann, Max-Born-Institute for Nonlinear Optics and Short-Pulse Spectroscopy, Berlin, Germany

Miguel A. Porras, Departamento de Física Aplicada, Escuela Técnica Superior de Ingenieros de Minas, Universidad Politécnica de Madrid, Madrid, Spain

Erasmo Recami, Facoltà di Ingegneria, Università degli Studi di Bergamo, Bergamo, Italy and INFN–Sezione di Milano, Milan, Italy

Kaido Reivelt, Institute of Physics, University of Tartu, Tartu, Estonia

Peeter Saari, Institute of Physics, University of Tartu, Tartu, Estonia

Janne Salo, Laboratory of Physics, Helsinki University of Technology, Espoo, Finland

Amr M. Shaarawi, Department of Physics, The American University of Cairo, Cairo, Egypt

Günter Steinmeyer, Max-Born-Institute for Nonlinear Optics and Short-Pulse Spectroscopy, Berlin, Germany

Gero Stibenz, Max-Born-Institute for Nonlinear Optics and Short-Pulse Spectroscopy, Berlin, Germany

Grover A. Swartzlander, Jr., College of Optical Sciences, University of Arizona, Tucson, Arizona

Stefano Trillo, Department of Engineering, University of Ferrara, Ferrara, Italy, and Research Center SOFT INFM-CNR, University La Sapienza, Rome, Italy

Michel Zamboni-Rached, Centro de Ciências Naturais e Humanas, Universidade Federal do ABC, Santo André, SP, Brazil

Preface

Diffraction and dispersion effects have been well known for centuries and are recognized to be limiting factors in many industrial and technology applications based, for example, on electromagnetic beams and pulses. Diffraction is an always-present phenomenon, affecting two- or three-dimensional waves traveling in nonguiding media. Arbitrary pulses and beams contain plane-wave components that propagate in different directions, causing a progressive increase in their spatial width along propagation. Dispersion is due to the dependence of the material media (refractive index) with frequency: therefore, each pulse's spectral component propagates with a different phase velocity, so that an electromagnetic pulse will suffer a progressive increase in its temporal width along propagation. It is clear that these two effects may be a serious restriction for applications where it is highly desirable that the beam keeps its transverse localization or the pulse keeps its transverse localization and/or temporal width along propagation, which might be desirable, for example, in free-space microwave, millimetric wave, terahertz and optical communications, microwave and optical images, optical lithography, and optical tweezers. As a consequence, the development of techniques capable of alleviating signal degradation effects caused by these two effects is of crucial importance.

Localized waves, also known as nondiffractive waves, arose initially as an attempt to obtain beams and pulses capable of resisting diffraction in free space for long distances. Such waves were obtained initially theoretically as solutions to the wave equation in the early 1940s (J. A. Stratton, *Electromagnetic Theory*, McGraw-Hill, New York, 1941), and were demonstrated experimentally in 1987 (J. Durnin, J. J. Miceli, and J. H. Eberly, Diffraction-free beams, *Phys. Rev. Lett.*, vol. 58, pp. 1499–1501, 1987). Nowadays localized waves constitute a growing and dynamic research topic, not only in relation to nondispersive free space (or vacuum), but also for dispersive, nonlinear, and lossy nonguiding media. Taking into account the significant amount of exciting and impressive results published especially in the last five years or so, we decided to edit a book on this topic, the first of its kind in the literature. The book is composed of 13 chapters authored by the most productive researchers in the field, with a well-balanced presentation of theory and experiment.

In Chapter 1, Recami et al. present a thorough review of localized waves, emphasizing the theoretical foundations along with historical aspects and the interconnections of this subject with other technology and scientific areas.

In Chapter 2, Zamboni-Rached et al. discuss in detail the theoretical structure of localized waves, and some applications are presented, among which frozen waves are of particular interest.

In Chapter 3, Besieris and Shaarawi present a hybrid spectral representation method which permits a smooth transition between two seemingly disparate classes of finite-energy spatiotemporally localized wave solutions to the three-dimensional scalar wave equation in free space: superluminal (X-shaped) and luminal (FWM-type) pulsed waves. An additional advantage of the hybrid form is that it obviates the presence of backward wave components, propagating at the luminal speed c, that have to be minimized in practical applications. A modified hybrid spectral representation method has also been presented which permits a seamless transition from superluminal localized waves to exact luminal splash modes. Within the framework of a certain parametrization, the latter are rendered indistinguishable from the paraxial luminal finite-energy-focused pulsed beam solutions.

In Chapter 4, Jian-yu Lu describes X-waves in depth, providing generalized methods for obtaining such waves through proper transformations, related primarily to the Lorentz transformation. X-wave solutions to Schrödinger and Klein–Gordon equations are also provided. In addition, the potential application of X-waves in medical ultrasound imaging is demonstrated experimentally.

In Chapter 5, Salo and Friberg show theoretically that diffraction-free wave propagation can also be achieved in anisotropic crystalline media. They explicitly analyze the effect of arbitrary anisotropies on both continuous-wave and pulsed nondiffracting fields. Due to beam steering and other effects, generation of nondiffracting waves in anisotropic media poses new challenges, and the authors propose an efficient scheme for the generation and detection of a continuous-wave beam in a crystal wafer.

In Chapter 6, Mugnai and Mochi explore Bessel X-waves' ability to provide localized energy and to exhibit superluminal propagation in both phase and group velocities (as verified experimentally). The authors also describe the ability of such waves to travel through a classically forbidden region (tunneling region) with no shift in the direction of propagation, which makes them different and unique with respect to ordinary waves.

In Chapter 7, Reivelt and Saari focus on the physical nature and experimental implementation or generation of localized waves. The authors demonstrate that the angular spectrum representation and the tilted pulse representation of localized waves are suitable tools for achieving these purposes. They explain the concepts and results of their experiments, where the realizability of Bessel X-waves and focus wave modes was verified for the first time.

In Chapter 8, Porras et al. present an interesting discussion of linear bullets, three-dimensional localized waves or particlelike waves propagating across a host medium, defeating diffraction spreading and dispersion broadening. Special attention is given to the generation of these bullets in practical settings by optical devices or by nonlinear means, showing the intimate relation between linear and nonlinear approaches to wave

bullets, as in light filaments. The advantage of linear bullets with respect to standard wave packets (Gaussian-like) is also demonstrated for a variety of applications, such as laser writing in thick media, ultraprecise microhole drilling for photonic-crystal fabrication, and laser micromachining.

In Chapter 9, the theory of X-waves in nonlinear materials is discussed thoroughly by Conti and Trillo. Potential applications in light-matter interactions at high laser intensities in quantum optics and on the theoretical prediction of X-waves in Bose–Einstein condensates are pointed out.

In Chapter 10, by Kukhlevsky, the problem of spatial localization of light in free space on a nanometer scale is presented in detail. The author shows that a sub-wavelength nanometer-sized beam propagating without diffractive broadening can be produced by the interference of multiple beams of a Fresnel light source of the respective material waveguide. The results demonstrate theoretically the feasibility of diffraction-free subwavelength-beam optics on a nanometer scale for both continuous waves and ultrashort (near-single-cycle) pulses. The approach extends the operational principle of near-field subwavelength-beam optics, such as near-field scanning optical microscopy, to the "not-too-distant" field regime (up to about 0.5 wavelength). The chapter includes theoretical illustrations to facilitate an understanding of the natural spatiotemporal broadening of light waves and the physical mechanisms that contribute to the diffraction-free propagation of subwavelength beams in free space.

In Chapter 11, Grunwald et al. show experimentally that ultraflat thin-film axicons enable the real physical approximation of nondiffracting beams and X-pulses of extremely narrow angular spectra. By self-apodized truncation of Bessel–Gauss pulses (coincidence of first field minimum with the rim of an aperture), needle-shaped propagation zones of large axial extension can be obtained without additional diffraction effects. The signature of undistorted progressive waves was indicated for such needle beams by the fringe-free propagation characteristics and ultrabroadband spatio-spectral transfer functions.

In Chapter 12, Longhi and Janner provide a general overview of wave localization (in a weak sense) for an important and novel class of inhomogeneous periodic dielectric media (i.e., in photonic crystals), which have received increasing attention in recent years. Compared to wave localization in homogeneous media, such as in a vacuum, the presence of a periodic dielectric permittivity strongly modifies the space–time dispersion surfaces and hence the types of localized waves that may be observed in photonic crystals.

In Chapter 13, Bouchal et al. focus on theoretical and experimental problems of nondiffracting and singular optics. Particular attention is devoted to physical properties, methods of experimental realization, and potential applications of single and composed vortex fields carried by a pseudo-nondiffracting background beam. The unique propagation effects of vortex fields are pointed out, and consequences of their spiral phase singularities manifested by a transfer of the orbital angular momentum are also discussed. The complex vortex structures whose parameters and properties are controlled dynamically by a spatial light modulation provide advanced methods of encoding and recording of information and can be utilized effectively in optical manipulations. Spatially localized vortex structures can be extended into

nonstationary optical fields where novel spatiotemporal effects and applications can be expected.

Acknowledgments

The editors are grateful to all the contributors to this volume for their efforts in producing stimulating high-quality chapters in an area that is not yet well known outside the community of experts, always with the aim of making the area more easily accessible to interested physicists and engineers. For useful discussions they are grateful to, among others, R. Bonifacio, M. Brambilla, R. Chiao, C. Cocca, C. Conti, A. Friberg, G. Degli Antoni, F. Fontana, G. Kurizki, M. Mattiuzzi, P. Milonni, P. Saari, A. Shaarawi, R. Ziolkowski, M. Tygel, and L. Ambrosio.

Preparation of the manuscript was facilitated greatly by George J. Telecki, Rachel Witmer, and Angioline Loredo from Wiley; we thank them for their fine professional work. We are indebted to Kai Chang, Ioannis M. Besieris, and Richard W. Ziolkowski for their crucial and inspirational encouragement. We would also like to thank our wives: Marli de Freitas Gomes Hernández, Jane Marchi Madureira, and Marisa T. Vasconselos, for their continuous loving support.

<div align="right">The Editors</div>

CHAPTER FOUR

Ultrasonic Imaging with Limited-Diffraction Beams

JIAN-YU LU
The University of Toledo, Toledo, Ohio

4.1 INTRODUCTION

One type of limited-diffraction beam was first described by Stratton in 1941as *undistorted progressive waves* (UPWs) [1]. In 1987, without referring to Stratton's work, Durnin et al. studied UPWs both by computer simulation and as an optical experiment [2–4]. Because the UPWs in Stratton's book have a Bessel transverse beam profile, they are termed *Bessel beams*. Durnin et al. named the Bessel beams *nondiffracting* or *diffraction-free beams* [2–4]. Because Durnin's terminology is controversial in the scientific community, these beams are commonly termed *limited-diffraction beams* [5], since all practical beams or waves will eventually diffract. Bessel beams are localized in the transverse direction and may have potential applications [6–14]. In acoustics, the first Bessel annular array transducer was designed and constructed in 1990 [15–16] and patented in 1992 [17]. Applications of Bessel beams in acoustics have been studied extensively [18–30].

Localized waves (LWs) were developed by Brittingham in 1983 and termed *focus wave modes* [31]. LWs have properties similar to those of Bessel beams in terms of transverse localization. In addition, LWs contain multiple frequencies and may be localized in the axial direction. LWs have been studied by many investigators

97

[32–40]. However, LWs are not propagation invariant; that is, they do not meet the propagation-invariant condition as defined in the following: If one travels with the wave at a speed c_1, he or she sees a wave packet, $\Phi(\vec{r}, t) = \Phi(x, y, z - c_1 t)$, that is unchanged for $z - c_1 t =$ constant, where z is the axial axis along the direction of wave propagation, $\vec{r} = (x, y, z)$ is a point in space, and t is the time.

To find multiple-frequency waves that are propagation invariant [i.e., $\Phi(\vec{r}, t) = \Phi(x, y, z - c_1 t)$], in 1991, X-waves were developed [41–43] and were studied subsequently [44–54]. The name X-waves was used because the beam profile in the axial cross section (a plane through the beam axis) resembles the letter "X." Due to the interest in X-waves for nonlinear optics and other applications, X-waves were introduced in 2004 in the "Search and Discovery" column of *Physics Today* [55]. The two 1992 X-wave papers [42–43] were awarded by the Ultrasonics, Ferroelectrics, and Frequency Control (UFFC) Society of the Institute of Electrical and Electronics Engineers (IEEE) in 1993. Later, an X-wave experiment in optics was performed by Saari and Reivelt and published in 1997 in *Physical Review Letters* [56]. To generalize X-waves, a transformation that is used to obtain limited-diffraction beams (including X-waves) in an *N*-dimensional space from any solutions to an $(N - 1)$-dimensional isotropic/homogeneous wave equation was developed in 1995 [44], where $N \geq 2$ is an integer. This formula has been related to part of the Lorentz transformation [57–58], and was used and demonstrated by other researchers [59–60]. Furthermore, an X-wave transform that is a transformation pair was developed in 2000 for any physically realizable waves using the orthogonal property of X-waves [46–47]. The orthogonal property of X-waves was studied further by Salo et al. in 2001 [61]. The transformation pair allows one to decompose an arbitrary physically realizable wave into X-waves (inverse X-wave transform) and determine the coefficients (forward X-wave transform) of the decomposition. Based on X-wave theory, a method and its extension that are capable of ultrahigh frame rate (HFR) two- or three-dimensional imaging were developed in 1997 [62–87]. Due to the importance of this method, it was noted as one of the predictions of the twenty-first century medical ultrasonics in 2000 [88]. After the introduction of X-waves in 1991 [41–43], these waves have been studied extensively by many investigators [56,58–60,89–123]. There are also some review papers on X-waves and their applications [124–131].

In this chapter, fundamentals of limited-diffraction beams are reviewed and studies of these beams are put into a unified theoretical framework. The theory of limited-diffraction beams is developed further. New limited-diffraction solutions to the Klein–Gordon and Schrödinger equations as well as limited-diffraction solutions to these equations in confined spaces are obtained. The relationship between the transformation that converts any solutions to an $(N-1)$-dimensional wave equation to limited-diffraction solutions of an *N*-dimensional equation and the Lorentz transformation is clarified and extended. The transformation is also applied to the Klein–Gordon equation. In addition, some applications of limited-diffraction beams are summarized.

4.2 FUNDAMENTALS OF LIMITED-DIFFRACTION BEAMS

4.2.1 Bessel Beams

An *N*-dimensional isotropic/homogeneous wave equation is given by

$$\left(\sum_{j=1}^{N} \frac{\partial^2}{\partial x_j^2} - \frac{1}{c^2} \frac{\partial^2}{\partial t^2} \right) \Phi(\vec{r}, t) = 0, \tag{4.1}$$

where $x_j (j = 1, 2, \ldots, N)$ represents rectangular coordinates in an *N*-dimensional space, $N \geq 1$ is an integer, $\Phi(\vec{r}, t)$ is a scalar function (sound pressure, velocity potential, or Hertz potential in electromagnetics) of spatial variables, $\vec{r} = (x_1, x_2, \ldots, x_N)$, t is time, and c is the speed of light in vacuum or the speed of sound in a medium.

In three–dimensional space, we have

$$\left(\nabla^2 - \frac{1}{c^2} \frac{\partial^2}{\partial t^2} \right) \Phi(\vec{r}, t) = 0, \tag{4.2}$$

where ∇^2 is the Laplace operator. In cylindrical coordinates, the wave equation is given by

$$\left[\frac{1}{r} \frac{\partial}{\partial r} \left(r \frac{\partial}{\partial r} \right) + \frac{1}{r^2} \frac{\partial^2}{\partial \phi^2} + \frac{\partial^2}{\partial z^2} - \frac{1}{c^2} \frac{\partial^2}{\partial t^2} \right] \Phi(\vec{r}, t) = 0, \tag{4.3}$$

where $r = \sqrt{x^2 + y^2}$ is the radial distance, $\phi = \tan^{-1}(y/x)$ is the polar angle, and z is the axial axis.

One generalized solution to the *N*-dimensional wave equation (4.1) is given by [42,124]

$$\Phi(x_1, x_2, \ldots, x_N; t) = f(s), \tag{4.4}$$

where

$$s = \sum_{j=1}^{N-1} D_j x_j + D_N (x_N \pm c_1 t), \qquad N \geq 1 \tag{4.5}$$

and where D_j are complex coefficients, $f(s)$ is any well-behaved complex function of s, and

$$c_1 = c \sqrt{\frac{1 + \sum_{j=1}^{N-1} D_j^2}{D_N^2}}. \tag{4.6}$$

If c_1 is real, $f(s)$ and its linear superposition represent limited-diffraction solutions to the N-dimensional wave equation (4.1). For example, if $N = 3$, $x_1 = x$, $x_2 = y$, $x_3 = z$, $D_1 = \alpha_0(k, \zeta) \cos \theta$, $D_2 = \alpha_0(k, \zeta) \sin \theta$, and $D_3 = b(k, \zeta)$, with cylindrical coordinates, we obtain families of solutions to (4.3) [42,124]:

$$\Phi_\zeta(s) = \int_0^\infty T(k) \left[\frac{1}{2\pi} \int_{-\pi}^{\pi} A(\theta) f(s) \, d\theta \right] dk \tag{4.7}$$

and

$$\Phi_K(s) = \int_{-\pi}^{\pi} D(\zeta) \left[\frac{1}{2\pi} \int_{-\pi}^{\pi} A(\theta) f(s) \, d\theta \right] d\zeta, \tag{4.8}$$

where

$$s = \alpha_0(k, \zeta) r \cos(\phi - \theta) + b(k, \zeta) \left[z \pm c_1(k, \zeta) t \right], \tag{4.9}$$

$$c_1(k, \zeta) = c\sqrt{1 + [\alpha_0(k, \zeta)/b(k, \zeta)]^2}, \tag{4.10}$$

$\alpha_0(k, \zeta)$, $b(k, \zeta)$, $A(\theta)$, $T(k)$, and $D(\zeta)$ are well-behaved functions, and θ, k, and ζ are free parameters. If $c_1(k, \zeta)$ is real and is not a function of k and ζ, respectively, $\Phi_\zeta(s)$ and $\Phi_K(s)$ are families of limited-diffraction solutions to the wave equation (4.3).

The following function is also a family of limited-diffraction solution to the wave equation [42,124]:

$$\Phi_L(r, \phi, z - ct) = \Phi_1(r, \phi) \Phi_2(z - ct), \tag{4.11}$$

where $\Phi_2(z - ct)$ is any well-behaved function of $z - ct$ and $\Phi_1(r, \phi)$ is a solution to the transverse Laplace equation:

$$\left[\frac{1}{r} \frac{\partial}{\partial r} \left(r \frac{\partial}{\partial r} \right) + \frac{1}{r^2} \frac{\partial^2}{\partial \phi^2} \right] \Phi_1(r, \phi) = 0. \tag{4.12}$$

If $T(k) = \delta(k - k')$, $f(s) = e^s$, $\alpha_0(k, \zeta) = -i\alpha$, and $b(k, \zeta) = i\beta$ in (4.7) and (4.9), we have

$$\Phi_\zeta(s) = \left[\frac{1}{2\pi} \int_{-\pi}^{\pi} A(\theta) e^{-i\alpha r \cos(\phi - \theta)} \, d\theta \right] e^{i(\beta z - \omega t)}, \tag{4.13}$$

where $\beta = \sqrt{k'^2 - \alpha^2}$ is the propagation parameter, $\delta(k - k')$ is the Dirac delta function, $k' = \omega/c > 0$ is the wave number, and ω is the angular frequency. If $A(\theta) = i^n e^{in\theta}$, one obtains an nth-order Bessel beam [2–4,15–17]:

$$\begin{aligned} \Phi_{B_n}(\vec{r}, t) &= \Phi_{B_n}(r, \phi, z - c_1 t) \\ &= e^{in\phi} J_n(\alpha r) e^{i(\beta z - \omega t)}, \qquad n = 0, 1, 2, \ldots, \end{aligned} \tag{4.14}$$

where the subscript B_n represents an nth-order Bessel beam, α is a scaling parameter, $J_n(\cdot)$ is an nth-order Bessel function of the first kind, and $c_1 = \omega/\beta$ is the phase velocity of the wave. It is clear that Bessel beams are single-frequency waves and are localized in the transverse direction. The scaling parameter, α, determines the degree of localization. Because of this property, Bessel beams can be applied to medical ultrasonic imaging [15–21]. Bessel beams are studied further [22–30] along with the studies of acoustic transducers and ultrasound waves [132–135].

4.2.2 Nonlinear Bessel Beams

In medical imaging, nonlinear properties are important to provide additional information on diseased tissues. Harmonics of Bessel beams due to the tissue nonlinearity are useful to obtain higher-quality images by combining the localized properties of limited-diffraction beams [22,23].

4.2.3 Frozen Waves

It is clear from (4.14) that single-frequency Bessel beams have two free parameters. One is the order of the Bessel function, and the other is the scaling parameter that changes the phase velocity of the Bessel beams. The order of the Bessel beams, n, in (4.14) has been exploited to produce various limited-diffraction beams of different transverse beam profiles since 1995 [29,30]. Another parameter, the scaling parameter, α, in (4.14), has also been used for a linear superposition of Bessel beams to produce a beam of a desired axial profile [24–27] for zeroth-order Bessel beams. Although an annular array was used in the production of superposed Bessel beams in these studies, the number of annuli and the width of each ring are free to change. When the number of annuli approaches infinity and the width of each ring shrinks to zero with a given circular aperture, the field distribution at the surface of the annular array is in fact a continuous function. In a more general way, one could use X-wave transform [28,46,47] to produce a wave whose shape would be close to the shape desired under conditions such as the least-squares criterion [136] by changing both the order of the beams and the scaling parameter.

In 2004, Zamboni-Rached developed an analytical relationship between the scaling parameter of Bessel beams and the axial beam profile along the beam axis ($r = 0$) for the zeroth-order Bessel beams. The resulting linear superposition of Bessel beams of different scaling parameter, α, was called *frozen waves* [137]. The method was extended to include superposition over both the scaling parameter and the order of the Bessel beams [138] to better control the transverse beam profile of the frozen waves. These studies not only provide computationally efficient ways for beam designs but may also have applications in optical tweezers [139].

4.2.4 X-Waves

If $T(k) = B(k)e^{-a_0 k}$, $A(\theta) = i^n e^{in\theta}$, $\alpha_0(k, \zeta) = -ik \sin \zeta$, $b(k, \zeta) = ik \cos \zeta$, and $f(s) = e^s$, one obtains an nth-order X-wave [41–53], which is a superposition of

limited-diffraction portion of axicon beams [140,141]:

$$
\begin{aligned}
\Phi_{X_n}(\vec{r}, t) &= \Phi_{X_n}(r, \phi, z - c_1 t) \\
&= e^{in\phi} \int_0^\infty B(k) J_n(kr \sin \zeta) e^{-k[a_0 - i \cos \zeta(z - c_1 t)]} \, dk, \qquad n = 0, 1, 2, \ldots,
\end{aligned}
$$
(4.15)

where the subscript X_n represents an nth-order X-wave, $c_1 = c/\cos \zeta \geq c$ is both the phase and group velocity of the wave, $|\zeta| < \pi/2$ is the axicon angle [141,142], a_0 is a positive free parameter that determines the decaying speed of the high-frequency components of the wave, and $B(k)$ is an arbitrary well-behaved transfer function of a device (acoustic transducer or electromagnetic antenna) that produces the wave. Comparing (4.15) with (4.14), it is easy to see the similarity and difference between a Bessel beam and an X-wave. X-waves are multiple-frequency waves, whereas Bessel beams have a single frequency. However, both waves have the same limited-diffraction property (i.e., they are propagation invariant). Because of multiple frequencies, X-waves can be localized in both transverse space and time to form a tight wave packet. They can propagate in free space or isotropic/homogeneous media without spreading or dispersion. Choosing specific $B(k)$, one can obtain analytical X-wave solutions [41–43]. One example is the zeroth-order [$n = 0$ and $B(k) = a_0$] X-wave [42]:

$$
\begin{aligned}
\Phi_{X_0}(\vec{r}, t) &= \Phi_{X_0}(r, \phi, z - c_1 t) \\
&= \int_0^\infty a_0 J_0(kr \sin \zeta) e^{-k[a_0 - i \cos \zeta(z - c_1 t)]} \, dk \\
&= \frac{a_0}{\sqrt{(r \sin \zeta)^2 + [a_0 - i \cos \zeta(z - c_1 t)]^2}}.
\end{aligned}
$$
(4.16)

4.2.5 Obtaining Limited-Diffraction Beams with Variable Transformation

If $\Phi_{N-1}(\vec{r}_{N-1}, t)$ is a solution to the $(N-1)$-dimensional isotropic/homogeneous wave equation, one can always obtain a limited-diffraction solution, $\Phi_N(\vec{r}_N, t)$, to the N-dimensional wave equation [see (4.1)] with the following variable substitutions [44]:

$$
\begin{array}{ccc}
\vec{r}_{N-1} \sin \zeta \to \vec{r}_{N-1} & & \vec{r}_{N-1} \sin \zeta \to \vec{r}_{N-1} \\
\dfrac{x_N \cos \zeta}{c} - t \to t & \text{or} & t - \dfrac{x_N \cos \zeta}{c} \to t,
\end{array}
$$
(4.17)

where $\vec{r}_{N-1} = (x_1, x_2, \ldots, x_{N-1})$, $\vec{r}_N = (x_1, x_2, \ldots, x_N)$, $N \geq 2$ is an integer, and $|\zeta| < \pi/2$ is the axicon angle [141,142] [for $N = 1$, $\Phi_{N-1}(\vec{r}_{N-1}, t) = \Phi_0(t)$ is a vibration and not a wave; in this case, (4.17) and the procedure above work only when $\zeta = 0$]. Because $x_N \cos \zeta/c - t$ appears as a single variable in the equation

$$
\Phi_N(\vec{r}_N, t) = \Phi_N(\vec{r}_{N-1}, x_N - c_1 t) = \Phi_{N-1}(\vec{r}_{N-1} \sin \zeta, x_N \cos \zeta/c - t), \quad (4.18)
$$

$\Phi_N(\vec{r}_N, t)$ is a limited-diffraction beam propagating along the axis, x_N. As shown in [57,58], (4.17) is related to part of the Lorentz transformation (missing the transformation on x_N) after dividing all variables by the same constant, $\sin \zeta$:

$$\frac{t}{\sin \zeta} - \frac{x_n \cos \zeta}{c \sin \zeta} = \frac{1}{\sin \zeta}\left(t - \frac{x_n \cos \zeta}{c}\right) = \gamma\left(t - \frac{\beta}{c}x_n\right) \overset{\vec{r}_{n-1} \to \vec{r}_{n-1}}{\to} t, \quad (4.19)$$

where $\beta = \cos \zeta = v/c$ and $\gamma = 1/\sin \zeta = 1/\sqrt{1 - \beta^2}$, and where $0 \leq v < c$ is the velocity of the moving coordinates (observer) along the axis, x_N. Contrary to the report in [57,58], if $\Phi_{N-1}(\vec{r}_{N-1}, t)$ is a solution to the $(N-1)$-dimensional isotropic/homogeneous wave equation, $\Phi_N(\vec{r}_N, t)$ will not be a solution to the N-dimensional wave equation (4.1) with the partial Lorentz transformation (4.19). Equation (17) has also been used in [59,60] to derive limited-diffraction beams in waveguides.

4.2.6 Limited-Diffraction Solutions to the Klein–Gordon Equation

An N-dimensional Klein–Gordon equation for a free relativistic particle is given by [143]:

$$\left(\sum_{j=1}^{N} \frac{\partial^2}{\partial x_j^2} - \frac{1}{c^2}\frac{\partial^2}{\partial t^2} - \frac{m^2 c^2}{\hbar^2}\right)\Phi_N(\vec{r}_N, t) = 0, \quad (4.20)$$

where $x_j(j = 1, 2, \ldots, N)$ represents rectangular coordinates in an N-dimensional space; $N \geq 1$ is an integer; $\Phi_N(\vec{r}_N, t)$ is a scalar wave function of spatial variables $\vec{r}_N = (x_1, x_2, \ldots, x_N)$ and time t; c is the speed of light in vacuum; $\hbar = h/2\pi$, where h is the Planck constant; $m = m' \sin \zeta$ is the mass of the particle at rest, where m' is a mass-related constant; and $|\zeta| < \pi/2$ is the axicon angle [141,142].

Assuming that $\Phi_{N-1}(\vec{r}_{N-1}, t)$ is a solution to the following $(N-1)$-dimensional Klein–Gordon equation with a mass m' [143]:

$$\left(\sum_{j=1}^{N-1} \frac{\partial^2}{\partial x_j^2} - \frac{1}{c^2}\frac{\partial^2}{\partial t^2} - \frac{m'^2 c^2}{\hbar^2}\right)\Phi_{N-1}(\vec{r}_{N-1}, t) = 0, \quad (4.21)$$

where $\vec{r}_{N-1} = (x_1, x_2, \ldots, x_{N-1})$; (4.18) is a solution to (4.20) after the variable substitution (4.17). This can be proved easily in a manner similar to that described in [44]. Using (4.18) and (4.21), we have

$$\left(\sum_{j=1}^{N-1} \frac{\partial^2}{\partial x_j^2}\right)\Phi_{N-1}\left(\vec{r}_{N-1}\sin \zeta, \frac{x_N \cos \zeta}{c} - t\right)$$

$$= \sin^2 \zeta\left(\frac{1}{c^2}\frac{\partial^2}{\partial t^2} + \frac{m'^2 c^2}{\hbar^2}\right)\Phi_{N-1}\left(\vec{r}_{N-1}\sin \zeta, \frac{x_N \cos \zeta}{c} - t\right) \quad (4.22)$$

and

$$\frac{\partial^2}{\partial x_N^2} \Phi_{N-1} \left(\vec{r}_{N-1} \sin \zeta, \frac{x_N \cos \zeta}{c} - t \right)$$

$$= \frac{\cos^2 \zeta}{c^2} \frac{\partial^2}{\partial t^2} \Phi_{N-1} \left(\vec{r}_{N-1} \sin \zeta, \frac{x_N \cos \zeta}{c} - t \right). \tag{4.23}$$

Summing both the left- and right-hand sides of (4.22) and (4.23), and comparing the results with (4.20), it is clear that (4.18) is a solution to (4.20). Limited-diffraction solutions to the Klein–Gordon equation mean that a free relativistic particle may be accompanied by a rigidly propagating wave along the axis, x_N, at a velocity that is greater than the speed of light in vacuum in a manner similar to that of X-waves [41–43] (for $\zeta \neq 0$). If $|\zeta| \to \pi/2$, the wave speed $c_1 = c/\cos \zeta \to \infty$ and then one has $m' \to m$. For photons where $m = 0$, (4.22) and (4.23) are the same as those in [44]. It is worth noting that from the proofs in (4.22) and (4.23) and in [44], it is clear that the functions $\sin \zeta$ and $\cos \zeta$ in (4.17) can be other functions as long as the summation of the squares of those functions is equal to 1: $f_1^2(\zeta) + f_2^2(\zeta) \equiv 1$, where $f_1(\zeta)$ and $f_2(\zeta)$ are any well-behaved functions of ζ or other free parameters. This extends the transformation formula in (4.17).

In the following we obtain some localized limited-diffraction solutions to the Klein–Gordon equation. Assuming that $f(s) = e^s$ in (4.4), where s is given by (4.5), and inserting (4.4) into (4.20), one obtains the velocity of the wave:

$$c_1 = c \sqrt{\frac{\left(\sum_{j=1}^{N} D_j^2 - m^2 c^2/\hbar^2 \right)}{D_N^2}}. \tag{4.24}$$

If $N = 3$, $x_1 = x$, $x_2 = y$, and $x_3 = z$, (4.24) becomes

$$c_1 = c \sqrt{\frac{\left(D_1^2 + D_2^2 + D_3^2 - m^2 c^2/\hbar^2 \right)}{D_3^2}}. \tag{4.25}$$

Choosing $D_1 = \alpha_0 \cos \theta$ and $D_2 = \alpha_0 \sin \theta$, where $-\pi \leq \theta \leq \pi$ is a free parameter and α_0 is a well-behaved function of any free parameters, if $\alpha_0 = -imc/\hbar \sin \zeta$, one obtains

$$D_3 = i \frac{mc}{\hbar} \left(\frac{\sqrt{1 - (\hbar/mc)^2 \alpha_0^2}}{\sqrt{(c_1/c)^2 - 1}} \right) = i \frac{mc}{\hbar} \frac{\sqrt{1 + \sin^2 \zeta}}{\sqrt{(c_1/c)^2 - 1}}. \tag{4.26}$$

Since e^s in (4.4) is a solution to the Klein–Gordon equation (4.20), a linear superposition over the free parameter, θ, is still a solution:

$$
\begin{aligned}
\Phi_{B_n}^{\mathrm{KG}}(\vec{r}, t) &= \frac{1}{2\pi} \int_{-\pi}^{\pi} A(\theta) e^s \, d\theta \\
&= e^{in\phi} J_n\left(\frac{mc}{\hbar} r \sin\zeta\right) \exp\left[i\frac{mc}{\hbar}\left(\frac{\sqrt{1 + \sin^2\zeta}}{\sqrt{(c_1/c)^2 - 1}} \right)(z - c_1 t) \right],
\end{aligned}
$$
$$(n = 0, 1, 2, \ldots), \quad (4.27)$$

where the subscript B_n and the superscript KG represent an nth-order Bessel beam and the Klein–Gordon equation, respectively, and $i(mc/\hbar)(\sqrt{1 + \sin^2\zeta}/\sqrt{(c_1/c)^2 - 1})$ is the propagation constant. Equation (4.27) is a localized solution to (4.20) and its localization increases with the mass, m. For electrons at rest, $m = 9.1 \times 10^{-31}$ kg, and thus $mc/\hbar = 2.6 \times 10^{12}$ m^{-1} ($\hbar = 1.05 \times 10^{-34}$ J·s and $c = 3.0 \times 10^8$ m/s). The wave in (4.27) is localized in picometer scale if $\sin\zeta \approx 1$. There are other choices of α_0. If α_0 is a constant, a localized limited-diffraction solution that has a fixed transverse beam profile can be obtained. If $\alpha_0 = -i(\gamma m v/\hbar)\sin\zeta$, where $\gamma = 1/\sqrt{1 - \beta^2}$ and $\beta = v/c$, and where v is the velocity of the particle, the transverse localization of the solutions will increase with the speed of the particle. In this case, the propagation constant is given by $i(mc/\hbar)(\sqrt{1 + (\gamma v/c)^2 \sin^2\zeta}/\sqrt{(c_1/c)^2 - 1})$.

Superposing $\Phi_{B_n}^{\mathrm{KG}}(\vec{r}, t)$ in (4.27) over the mass, m, one obtains a composed wave function that is similar to the X-wave [41–53] but may not necessarily be a solution to (4.20) where m is a constant for a given particle (the physical meaning could be a group of independent particles of different masses traveling in space). Using (4.7) and (4.27), and letting $T(k) = B(k)e^{-a_0 k}$, where $k = mc/\hbar$, one obtains

$$
\begin{aligned}
\Phi_{X_n}^{\mathrm{KG}}(\vec{r}, t) &= \Phi_{X_n}^{\mathrm{KG}}(r, \phi, z - c_1 t) \\
&= \frac{c}{\hbar} e^{in\phi} \int_0^\infty B\left(\frac{mc}{\hbar}\right) J_n\left(\frac{mc}{\hbar} r \sin\zeta\right) \\
&\quad \times \exp\left\{ \frac{mc}{\hbar}\left[a_0 - i\left(\sqrt{1 + \sin^2\zeta}/\sqrt{(c_1/c)^2 - 1} \right)(z - c_1 t) \right] \right\} dm,
\end{aligned}
$$
$$n = 0, 1, 2, \ldots, \quad (4.28)$$

where the subscript X_n represents an nth-order X-wave and the superscript KG the Klein–Gordon equation, a_0 is a positive free parameter, and $B(k)$ is an arbitrary well-behaved transfer function. If $n = 0$ and $B(k) = a_0$, from (4.28) and (4.16) one has (where c_1 is a constant) [42]

$$
\begin{aligned}
\Phi_{X_0}^{\mathrm{KG}}(\vec{r}, t) &= \Phi_{X_0}^{\mathrm{KG}}(r, \phi, z - c_1 t) \\
&= \frac{a_0}{\sqrt{(r\sin\zeta)^2 + \left[a_0 - i\left(\sqrt{1 + \sin^2\zeta}/\sqrt{(c_1/c)^2 - 1} \right)(z - c_1 t) \right]^2}}.
\end{aligned}
$$
$$(4.29)$$

It is clear from (4.26)–(4.29) that if $c_1 < c$, the solutions or functions are no longer waves. If $c_1 = c$, D_3 in (4.26) is infinity. For $c_1 > c$, one obtains rigidly propagating superluminal waves or functions, as in the case of X-waves [42]. One example is to assume that $c_1 = c/\cos\zeta$, as given in (4.17) [44]. A superposition that is similar to (4.28) can also be done over the velocity, v, instead of the mass, m, of a particle if, say, $\alpha_0 = -i(\gamma m v/\hbar)\sin\zeta$. In this case, the superposition is a limited-diffraction solution to the Klein–Gordon equation (4.20).

4.2.7   Limited-Diffraction Solutions to the Schrödinger Equation

The general nonrelativistic, time-dependent, and three-dimensional Schrödinger wave equation for multiple particles is given by (see, e.g., [144])

$$-\sum_{j=1}^{M}\frac{\hbar^2}{2m_j}\nabla_j^2\Phi + V\Phi = i\hbar\frac{\partial\Phi}{\partial t}, \tag{4.30}$$

where $\Phi = \Phi(x_1, x_2, x_3; \ldots; x_{3M-2}, x_{3M-1}, x_{3M}; t)$ is the wave function (related to the probability of finding particles in space and time) and $V = V(x_1, x_2, x_3; \ldots; x_{3M-2}, x_{3M-1}, x_{3M}; t)$ is the potential of the system. Φ and V are determined by all the particles and their interactions. ∇_j^2 is the Laplace in terms of the position of the jth particle in space, $\vec{r}_j = (x_{3j-2}, x_{3j-1}, x_{3j})$, where $j = 1, 2, \ldots, M$ (M is an integer) and m_j is the mass at rest of the jth particle. Assuming that V is not a function of spatial variables and time, and $\Phi(s) = e^s$, where s is given by (4.5), one obtains [54]

$$c_1 = \frac{\sum_{j=1}^{M}(-\hbar^2/2m_j)\left(D_{3j-2}^2 + D_{3j-1}^2 + D_{3j}^2\right) + V}{-i\hbar D_{3M}}. \tag{4.31}$$

If $M = 1, x_1 = x, x_2 = y, x_3 = z, m_1 = m, D_1 = \alpha_0\cos\theta$, and $D_2 = \alpha_0\sin\theta$, where $|\zeta| < \pi/2$ is an axicon angle, $-\pi \le \theta \le \pi$ is a free parameter, and α_0 is a well-behaved function of any free parameters, (4.31) is simplified [54] as

$$c_1 = \frac{(-\hbar^2/2m)\left(\alpha_0^2 + D_3^2\right) + V}{-i\hbar D_3}. \tag{4.32}$$

If $V = 0$ and $\alpha_0 = -i(mc/\hbar)\sin\zeta$, one has

$$D_3 = \begin{cases} i\dfrac{mc}{\hbar}\left(\dfrac{c_1}{c} \pm \sqrt{\left(\dfrac{c_1}{c}\right)^2 + \dfrac{\hbar^2}{m^2c^2}\alpha_0^2}\right) = i\dfrac{mc}{\hbar}\left(\dfrac{c_1}{c} \pm \sqrt{\left(\dfrac{c_1}{c}\right)^2 - \sin^2\zeta}\right), & \alpha_0 \ne 0 \\[4mm] i\cdot 2\dfrac{mc}{\hbar}\dfrac{c_1}{c}, & \alpha_0 = 0. \end{cases} \tag{4.33}$$

Following the steps to obtain (4.27), one obtains a localized solution to the Schrödinger equation in (4.30) under the conditions leading to (4.33) [54]:

$$
\begin{aligned}
\Phi_{B_n}^{S}(\vec{r}, t) &= \frac{1}{2\pi} \int_{-\pi}^{\pi} A(\theta) e^{s}\, d\theta \\
&= e^{in\phi} J_n\left(\frac{mc}{\hbar} r \sin\zeta\right) \exp\left[i \frac{mc}{\hbar}\left(c_1/c \pm \sqrt{(c_1/c)^2 - \sin^2\zeta}\right)(z - c_1 t)\right],
\end{aligned}
$$
$$n = 0, 1, 2, \ldots, \quad (4.34)$$

where the subscript B_n and the superscript S represent an nth-order Bessel beam and the Schrödinger equation, respectively, and $i(mc/\hbar)(c_1/c \pm \sqrt{(c_1/c)^2 - \sin^2\zeta})$ is the propagation constant. Similar to the Klein–Gordon equation [see the text below (4.27)], one can select $\alpha_0 = \text{constant}$, $\alpha_0 = -i(\gamma mv/\hbar)\sin\zeta$, or other functions to obtain more limited-diffraction beams [the corresponding D_3 can be obtained easily by inserting different α_0 into (4.33)].

Following the derivations of (4.28) and substituting $(mc/\hbar)(\sqrt{1 + \sin^2\zeta}/\sqrt{(c_1/c)^2 - 1})$ with $(mc/\hbar)(c_1/c \pm \sqrt{(c_1/c)^2 - \sin^2\zeta})$, one obtains a function that is similar to the X-wave [41–53] but may not necessarily be a solution to (4.30) (the physical meaning could be a group of independent particles of different masses traveling in space):

$$
\begin{aligned}
\Phi_{X_n}^{S}(\vec{r}, t) &= \Phi_{X_n}^{S}(r, \phi, z - c_1 t) \\
&= \frac{c}{\hbar} e^{in\phi} \int_0^{\infty} B\left(\frac{mc}{\hbar}\right) J_n\left(\frac{mc}{\hbar} r \sin\zeta\right) \\
&\quad \times \exp\left\{-\frac{mc}{\hbar}\left[a_0 - i\left(c_1/c \pm \sqrt{(c_1/c)^2 - \sin^2\zeta}\right)(z - c_1 t)\right]\right\} dm,
\end{aligned}
$$
$$n = 0, 1, 2, \ldots, \quad (4.35)$$

where the subscript X_n represents an nth-order X-wave and the superscript S represents the Schrödinger equation, a_0 is a positive free parameter, and $B(k)$ is an arbitrary well-behaved transfer function. If $n = 0$ and $B(k) = a_0$, from (4.35) and (4.16), one obtains (where c_1 is a constant) [42]

$$
\begin{aligned}
\Phi_{X_0}^{S}(\vec{r}, t) &= \Phi_{X_0}^{S}(r, \phi, z - c_1 t) \\
&= \frac{a_0}{\sqrt{(r \sin\zeta)^2 + \left[a_0 - i\left(c_1/c \pm \sqrt{(c_1/c)^2 - \sin^2\zeta}\right)(z - c_1 t)\right]^2}}.
\end{aligned}
\quad (4.36)
$$

In (4.33–4.36), if $(c_1/c)^2 - \sin^2\zeta < 0$, the solutions or functions are unbounded for some z or t and may not be of interest. If $(c_1/c)^2 - \sin^2\zeta \geq 0$, one obtains limited-diffraction solutions or functions [42]. One example is to assume that $c_1 = c/\cos\zeta$, as given in (4.17) [44]. A superposition that is similar to (4.35) can also be done over the velocity, v, instead of the mass, m, of a particle if, say, $\alpha_0 = -i(\gamma mv/\hbar)\sin\zeta$.

108   ULTRASONIC IMAGING WITH LIMITED-DIFFRACTION BEAMS

In this case, the superposition is a limited-diffraction solution to the Schrödinger equation (4.30).

4.2.8 Electromagnetic X-Waves

The free-space Maxwell's equations are given by [145]

$$\nabla \times \vec{E} = -\mu_0 \frac{\partial \vec{H}}{\partial t} \quad \nabla \cdot \vec{E} = 0$$
$$\nabla \times \vec{H} = \varepsilon_0 \frac{\partial \vec{E}}{\partial t} \qquad \nabla \cdot \vec{H} = 0, \tag{4.37}$$

where $\vec{E}$ is the electric field strength, $\vec{H}$ is the magnetic field strength, ε_0 is the dielectric constant of free space ($\varepsilon_0 \approx \pi/36 \times 10^{-9} F/m$), μ_0 is the magnetic permeability of free space ($\mu_0 = 4\pi \times 10^{-7}$H/m), and t is the time.

Because of the third equation ($\nabla \cdot \vec{E} = 0$) of (4.37), the electric field strength can be written [54,146]

$$\vec{E} = -\mu_0 \frac{\partial}{\partial t} \nabla \times \vec{\prod}_m, \tag{4.38}$$

where $\vec{\prod}_m = \Phi \vec{n}^0$ is a magnetic Hertz vector potential with transverse electrical (TE) polarization, where Φ is a scalar function and $\vec{n}^0$ represents a unit vector. Inserting (4.38) into the first equation of (4.37), one obtains

$$\vec{H} = \nabla \times \left(\nabla \times \vec{\prod}_m \right). \tag{4.39}$$

From (4.37–4.39), one obtains the vector wave equation

$$\nabla^2 \vec{\prod}_m - \frac{1}{c^2} \frac{\partial^2 \vec{\prod}_m}{\partial t^2} = 0. \tag{4.40}$$

Letting $\vec{n}^0 = \vec{z}^0$, where $\vec{z}^0$ is a unit vector along the z-axis, and using cylindrical coordinates from (4.38) and (4.39) we obtain

$$\vec{E} = -\mu_0 \frac{1}{r} \frac{\partial^2 \Phi}{\partial t \, \partial \phi} \vec{r}^0 + \mu_0 \frac{\partial^2 \Phi}{\partial t \, \partial r} \vec{\phi}^0 \tag{4.41}$$

and

$$\vec{H} = \frac{\partial^2 \Phi}{\partial r \, \partial z} \vec{r}^0 + \frac{1}{r} \frac{\partial^2 \Phi}{\partial \phi \, \partial z} \vec{\phi}^0 + \left(\frac{\partial^2 \Phi}{\partial z^2} - \frac{1}{c^2} \frac{\partial^2 \Phi}{\partial t^2} \right) \vec{z}^0, \tag{4.42}$$

respectively, where Φ is a solution to the free-space scalar wave equation (4.2), and where $\vec{r}^0$ and $\vec{\phi}^0$ are the unit vectors along the variables r and ϕ, respectively. Once

a solution to (4.2) is found, the electrical field strength, $\vec{E}$, and the magnetic field strength, $\vec{H}$, can be obtained from Eqs. (4.41) and (4.42), respectively.

If Φ is an nth-order broadband X-wave solution or a general X-wave solution [see (4.15)] to (4.2), the components of $\vec{E}$ and $\vec{H}$ are also X-wave functions [54]. From the $\vec{E}$ and $\vec{H}$ expressions, the Poynting energy flux vector and the energy density can be derived [54]. Solutions to $\vec{E}$ and $\vec{H}$ obtained this way will be limited-diffraction solutions to Maxwell's equations in (4.37) [54].

4.2.9 Limited-Diffraction Beams in Confined Spaces

Limited-diffraction beams in confined spaces are of interest [59,60,147]. Previously, Shaarawi et al. [148] and Ziolkowski et al. [149] have shown that localized waves such as focused wave modes and modified power spectrum pulses can also propagate in waveguides for an extended propagation depth. In the following, theoretical results of X-waves propagating in a confined space such as a waveguide are developed for acoustics, electromagnetics, and quantum mechanics [147].

1. *Acoustic waves.* Assuming that Φ in (4.2) represents acoustic pressure in an infinitely long cylindrical acoustical waveguide (radius a), which is filled with an isotropic/homogeneous lossless fluid medium enclosed in an infinitely rigid boundary, the normal vibration velocity of the medium at the wall of the cylindrical waveguide is zero for all the frequency components of the X-waves [i.e., $\partial \Phi_{X_n}(\vec{r}, t; \omega)/\partial r \equiv 0$, $\forall \omega \geq 0$ at $r = a$, where $\Phi_{X_n}(\vec{r}, t; \omega)$ is the X-wave component at angular frequency ω; see (4.15)]. To meet this boundary condition, the parameter k in (4.15) is quantized:

$$k_{nj} = \frac{\mu_{nj}}{a \sin \zeta}, \qquad n, j = 0, 1, 2, \ldots, \tag{4.43}$$

where μ_{nj} are the roots of the equations

$$\begin{aligned} J_1(x) &= 0, & n &= 0 \\ J_{n-1}(x) &= J_{n+1}(x), & n &= 1, 2, \ldots \end{aligned} \tag{4.44}$$

Thus, the integral in (4.15) can be changed to a series representing frequency-quantized X-waves [147]:

$$\Phi_{X_n}(\vec{r}, t) = e^{in\phi} \sum_{j=0}^{\infty} \Delta k_{nj} B(k_{nj}) J_n(k_{nj} r \sin \zeta) e^{-k_{nj}[a_0 - i \cos \zeta(z - c_1 t)]}, \qquad r \leq a,$$
$$n = 0, 1, 2, \ldots, \tag{4.45}$$

where $\Delta k_{n0} = k_{n1}$ and $\Delta k_{nj} = k_{nj+1} - k_{nj}$ $(j = 1, 2, 3, \ldots)$. Unlike conventional guided waves, frequency-quantized X-waves contain multiple frequencies and propagate through waveguides at the speed of c_1 without dispersion, and similar results can be obtained for waveguides of other homogeneous boundary conditions. For an
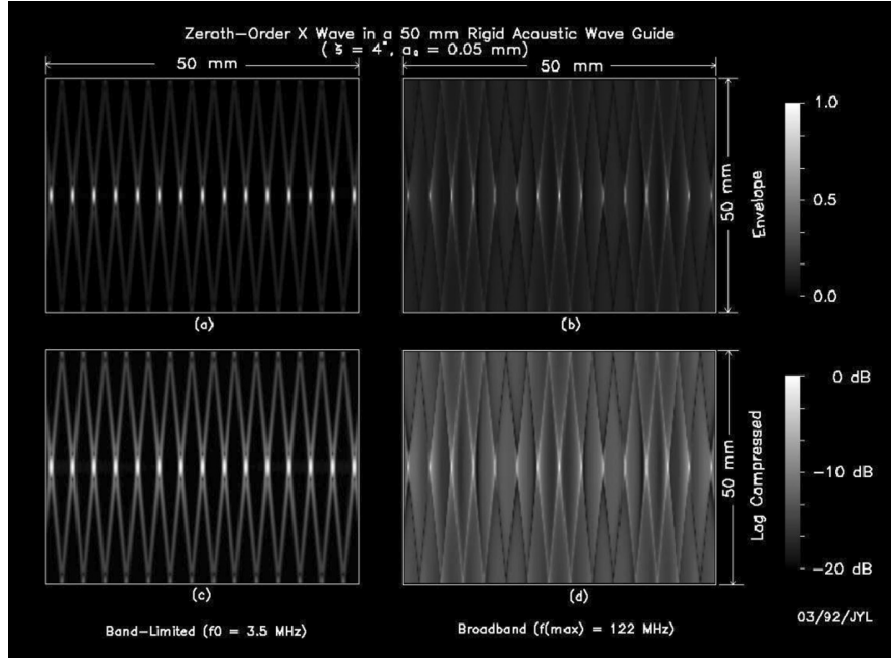
FIGURE 4.1   Envelope-detected zeroth-order X-wave in a 50 mm-diameter rigid acoustic waveguide. The waves shown has an axicon angle of $4°$ and $a_0 = 0.05$ mm. (a) and (c) Bandlimited version with a Blackman window function centered at 3.5 MHz with about 81% of fractional -6 dB bandwidth. (b) and (d) are broadband versions. The images in the top row are on a linear scale and those in the bottom row are of log scale, to show the sidelobes.

infinitely long cylindrical acoustical waveguide consisting of isotropic/homogeneous lossless media in a free space (vacuum) with radius a, the acoustical pressure is zero at the boundary of the waveguide, $r = a$ [i.e., $\mu_{nj}(n, j = 1, 2, 3, \ldots)$ in (4.43) are roots of $J_n(x) = 0 \, (j = 1, 2, \ldots)$]. See Figs. 4.1 to 4.3 for examples of X-waves in an acoustic waveguide [147].

It is clear that if $n = 0, (4.45)$ represents an axially symmetric frequency-quantized X-wave. If $a \to \infty$, $\Delta k_{nj} \to 0$ and the summation in (4.45) becomes an integration that represents the X-waves in (4.15). On the other hand, if $a \to 0$, both k_{nj} and $\Delta k_{nj} \to \infty$ $(n, j = 0, 1, 2, \ldots)$. This means that for a small waveguide, only high-frequency-quantized X-waves can propagate through it.

2. *Electromagnetic waves.* The free-space vector wave equations from the free-space Maxwell's equations (4.37) are given by [150]

$$\nabla^2 \vec{E} - \frac{1}{c^2} \frac{\partial^2 \vec{E}}{\partial t^2} = 0 \qquad (4.46)$$
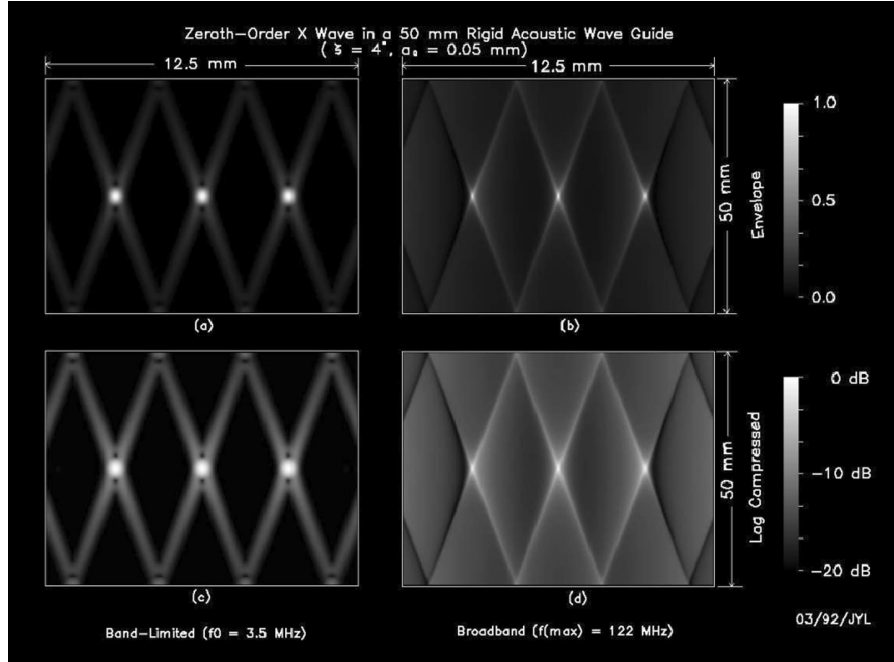
FIGURE 4.2   The same as those in Fig. 4.1 except that the images are zoomed horizontally around the center.

and

$$\nabla^2 \vec{H} - \frac{1}{c^2} \frac{\partial^2 \vec{H}}{\partial t^2} = 0. \tag{4.47}$$

A solution to (4.46) can be written as

$$\vec{E}(\vec{r}, t) = \vec{E}_\perp(r, \phi) e^{\gamma z - i\omega t}, \tag{4.48}$$

where $\gamma = i\beta$ is a propagation constant, $\beta = \sqrt{k^2 - k_c^2} > 0$ (for propagation waves), $k = \omega/c$ is the wave number, and $\vec{E}_\perp(r, \phi)$ is a solution of the transverse vector Helmholtz equation:

$$\nabla_\perp^2 \vec{E}_\perp(r, \phi) + k_c^2 \vec{E}_\perp(r, \phi) = 0, \tag{4.49}$$

where $\nabla_\perp^2$ is the transverse Laplace operator and k_c is a parameter that is independent of r, ϕ, z, and t. For transverse magnetic (TM) waves, $\vec{E}_\perp(r, \phi) = E_z(r, \phi)\vec{z}^0$ and (4.49) becomes a scalar Helmholtz equation of $E_z(r, \phi)$, where $\vec{z}^0$ is a unit vector along the z-axis.
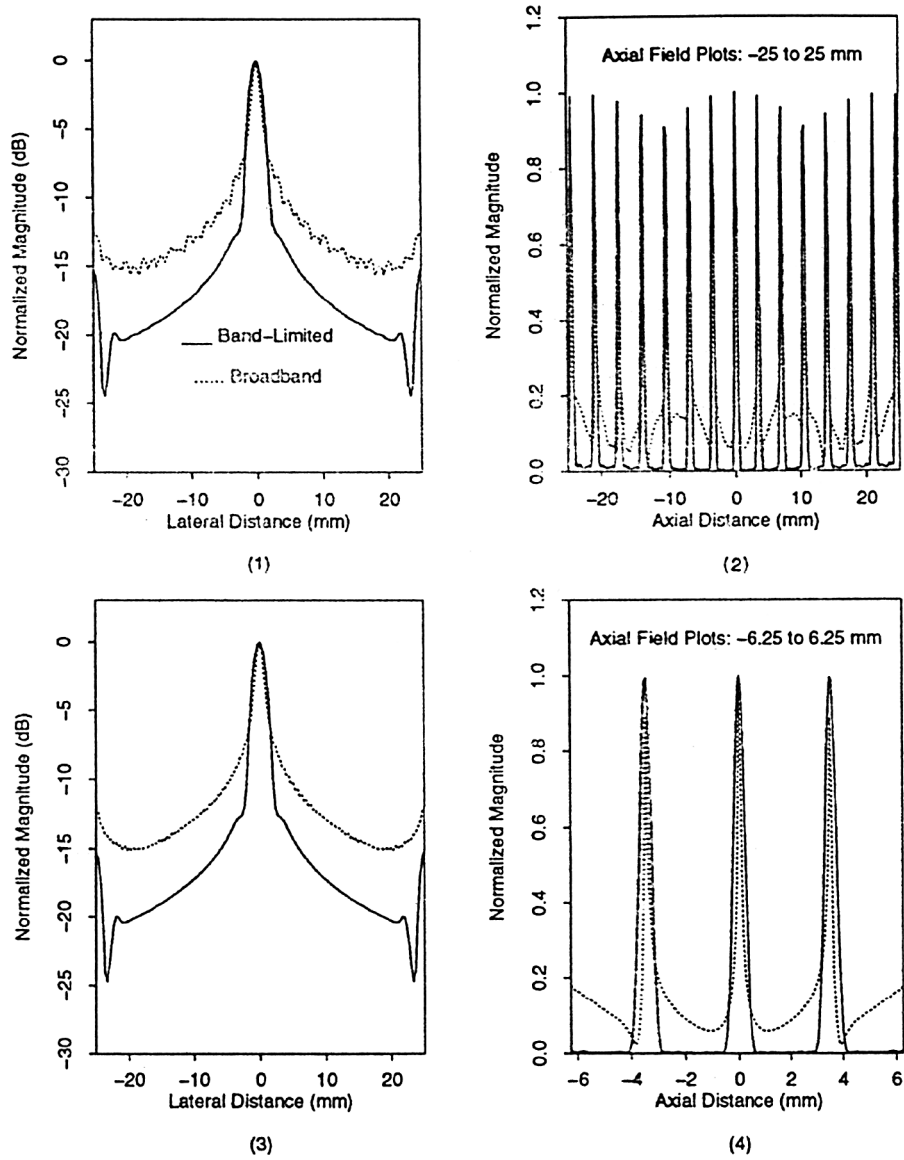
FIGURE 4.3   Transverse [(1) and (3)] and axial [(2) and (4)] sidelobe plots of the images in Fig. 4.1 [(1) and (2)] and Fig. 4.2 [(3) and (4)], respectively. Solid and dotted lines are for bandlimited and broadband cases, respectively.

If $k_c = k \sin \zeta$, where $|\zeta| < \pi/2$ is a constant, after taking into consideration the exponential term in (4.48) and integrating the solution of (4.49) from 0 to ∞ over k, one obtains an nth-order X-wave solution [replace the symbol, $\Phi_{X_n}(\vec{r}, t)$, in (4.15) with $E_{z_{n\mathrm{X}}}(\vec{r}, t)$, where the subscript X indicates an X-wave]. Assuming that electromagnetic X-waves travel in vacuum in a totally conductive cylindrical waveguide of a radius, a [i.e., $E_{z_{n\mathrm{X}}}(\vec{r}, t) \equiv 0$ at $r = a$], similar to the frequency quantization procedure of the acoustic case (4.45), one obtains [147]

$$E_{z_{n\mathrm{X}}}(\vec{r}, t) = e^{in\phi} \sum_{j=0}^{\infty} \Delta k_{nj} B(k_{nj}) J_n(k_{nj} r \sin \zeta) e^{-k_{nj}[a_0 - i \cos \zeta (z - c_1 t)]}, \qquad r \leq a,$$

$$n = 0, 1, 2, \ldots, \quad (4.50)$$

where the k_{nj} $(n, j = 0, 1, 2, \ldots)$ are given by (4.43) and the μ_{nj} $(n, j = 0, 1, 2, \ldots)$ in (4.43) are roots of $J_n(x) = 0$ $(n = 0, 1, 2, \ldots)$. Other components of $\vec{E}$ and $\vec{H}$ can be derived from $E_z(\vec{r}, t)$ using the free-space Maxwell's equations (4.37). They will have the same speed, c_1, as E_z. For transverse electric (TE) waves, the results are similar.

3. *DeBroglie waves.* With a finite transverse spatial extension (such as a free particle passing through a hole with a finite aperture), the function $\Phi_{X_n}^{\mathrm{KG}}(\vec{r}, t)$ in (4.28) or $\Phi_{X_n}^{\mathrm{S}}(\vec{r}, t)$ in (4.35) would change (spread or diffract) after certain distance behind the hole. However, in cases such as particles passing through a pipe, $\Phi_{X_n}^{\mathrm{KG}}(\vec{r}, t)$ and $\Phi_{X_n}^{\mathrm{S}}(\vec{r}, t)$ need to meet the boundary conditions that they are zero on the wall of the pipe. This gives the following quantized X-wave functions corresponding to (4.28) and (4.35), respectively [147]:

$$\Phi_{X_n}^{\mathrm{KG}}(\vec{r}, t) = e^{in\phi} \sum_{j=0}^{\infty} \Delta k_{nj} B(k_{nj}) J_n(k_{nj} r \sin \zeta) e^{-k_{nj}\left[a_0 - i\left(\sqrt{1+\sin^2 \zeta}/\sqrt{(c_1/c)^2 - 1}\right)(z - c_1 t)\right]},$$

$$r \leq a, \quad n = 0, 1, 2, \ldots, \quad (4.51)$$

and

$$\Phi_{X_n}^{\mathrm{S}}(\vec{r}, t) = e^{in\phi} \sum_{j=0}^{\infty} \Delta k_{nj} B(k_{nj}) J_n(k_{nj} r \sin \zeta) e^{-k_{nj}\left[a_0 - i\left(c_1/c \pm \sqrt{(c_1/c)^2 - \sin^2 \zeta}\right)(z - c_1 t)\right]},$$

$$r \leq a, \quad n = 0, 1, 2, \ldots, \quad (4.52)$$

where $k_{nj} = m_{nj} c / \hbar$ $(n, j = 0, 1, 2, \ldots)$ are given by (4.43) and μ_{nj} $(n, j = 0, 1, 2, \ldots)$ in (4.43) are roots of $J_n(x) = 0$ $(n = 0, 1, 2, \ldots)$. Equations (4.51) and (4.52) represent particles in a confined space with their quantized de Broglie's waves. The quantization may only allow particles of a certain mass to pass through the pipe (waveguide). As mentioned in the text below (4.27) and (4.34), the free parameter α_0 can be chosen differently. If $\alpha_0 = -i(\gamma m v / \hbar) \sin \zeta$, the quantization in (4.51) and (4.52) may be modified for summation over the velocity v, instead of m, of the

particles. In this case, only particles with certain velocities are allowed to pass through the pipe or a small nanotube.

There are other implications of the studies above. As we know, light in free space behaves like a wave but acts as particles (photons) when interacting with materials. Some microscopic structures of materials could be considered as optical waveguides within which the light waves are confined. From our discussion above of X-waves in confined spaces, it is understood that only light waves that have a higher energy (or frequency) can penetrate these materials or cause interactions.

4.2.10 X-Wave Transformation

Because X-waves are orthogonal [61], similar to plane waves, any physically realizable waves or well-behaved solutions to the wave equation can be expressed as a linear superposition of X-waves (inverse X-wave transform), and the coefficients of the superposition can be determined (forward X-wave transform), [46,47]. The inverse X-wave transform is given by (Eq. (4.15) of [46])

$$
\begin{aligned}
\Phi(\vec{r}, t) &= \sum_{n=-\infty}^{\infty} \int_0^{\pi/2} d\zeta \int_0^{\infty} dk\, T_{n,\zeta}(k) \Phi_{A_{n,k,\zeta}}(r, \phi, z - c_1 t) \\
&= \sum_{n=-\infty}^{\infty} \int_0^{\pi/2} \left[e^{in\phi} \int_0^{\infty} T_{n,\zeta}(k) J_n(kr \sin\zeta) e^{ik\cos\zeta(z-c_1 t)}\, dk \right] d\zeta \\
&= \sum_{n=-\infty}^{\infty} \int_0^{\pi/2} \Phi_{X_{n,\zeta}}(r, \phi, z - c_1 t)\, d\zeta,
\end{aligned}
\tag{4.53}
$$

where

$$
T_{n,\zeta}(k) = B_{n,\zeta}(k) e^{-ka_0}
\tag{4.54}
$$

and

$$
\Phi_{A_{n,k,\zeta}}(r, \phi, z - c_1 t) = e^{in\phi} J_n(kr \sin\zeta) e^{ik\cos\zeta(z-c_1 t)},
\tag{4.55}
$$

where $c_1 = c/\cos\zeta$ and $|\zeta| < \pi/2$.

The forward X-wave transform can be used to determine the coefficients (Eq. (4.26) of [46]):

$$
\begin{aligned}
T_{n,\zeta}(k) = {}& \frac{k^2 c \sin\zeta \cos\zeta\, H(k)}{(2\pi)^2} \\
& \times \int_0^{\infty} r\, dr \int_{-\pi}^{\pi} d\phi \int_{-\infty}^{\infty} dt\, \Phi(r, \phi, z, t) \Phi_{A_{n,k,\zeta}}^*(r, \phi, z - c_1 t),
\end{aligned}
\tag{4.56}
$$

where

$$\Phi^*_{A_{n,k,\zeta}}(r, \phi, z - c_1 t) = e^{-in\phi} J_n(kr \sin \zeta) e^{-ik \cos \zeta (z - c_1 t)} \tag{4.57}$$

is a complex conjugate of $\Phi_{A_{n,k,\zeta}}(r, \phi, z - c_1 t)$ and $H(k)$ is the Heaviside step function [151]:

$$H(k) = \begin{cases} 1, & k \geq 0 \\ 0, & \text{otherwise.} \end{cases} \tag{4.58}$$

$H(k)$ is used to indicate that k is positive and thus can be placed on either side of (56).

4.2.11 Bowtie Limited-Diffraction Beams

If $\Phi_N(\vec{r}_N, t) = \Phi_N(\vec{r}_{N-1}, x_N - c_1 t)$ is a limited-diffraction solution to the isotropic/homogeneous wave equation (4.1), the Klein–Gordon equation (4.20), or the Schrödinger equation (4.30) (assuming that V is not a function of the corresponding component of $\vec{r}_{N-1}$), where $\vec{r}_N = (x_1, x_2, \ldots, x_N)$, $\vec{r}_{N-1} = (x_1, x_2, \ldots, x_{N-1})$, N is an integer, and c_1 is the speed of the wave, any partial derivatives of $\Phi_N(\vec{r}_{N-1}, x_N - c_1 t)$ along any component of $\vec{r}_{N-1}$ are still limited-diffraction solutions to these equations [152–156]. These solutions are called *bowtie beams* because their transverse beam shapes are similar to the shape of a bowtie. These beams may have applications in medical imaging of a lower sidelobe because one part of the sidelobe of a transmission beam may be used to cancel the other part of the sidelobe of a reception beam [152–156]. [Note that the following properties are also true. Any partial derivatives of a limited-diffraction solution, $\Phi_N(\vec{r}_{N-1}, x_N - c_1 t)$, in terms of the time t will also be a limited-diffraction solution to (4.1), (4.20), and (4.30), respectively. One example is the second derivative X-wave in terms of time given in [44]. Replacing t with $-t$ in $\Phi_N(\vec{r}_{N-1}, x_N - c_1 t)$, one obtains a time-reversal mirror limited-diffraction wave propagating in a backward direction along x_N.]

4.2.12 Limited-Diffraction Array Beams

If the partial derivatives are carried out on more than one component of $\vec{r}_{N-1} = (x_1, x_2, \ldots, x_{N-1})$ for $\Phi_N(\vec{r}_N, t) = \Phi_N(\vec{r}_{N-1}, x_N - c_1 t)$, limited-diffraction grid or layered array beams may be produced for equations (4.1), (4.20), and (4.30) (assuming that V is not a function of the corresponding components of $\vec{r}_{N-1}$) [157–160]. Array beams may have applications to three-dimensional imaging [157], blood-flow velocity measurements [158], and high-frame-rate imaging [62,63,79–85].

4.2.13 Computation with Limited-Diffraction Beams

Efficient computation of limited-diffraction beams produced by a finite aperture is important for understanding the properties of these beams. A Fourier–Bessel method

[24–28] has been used to calculate arbitrary waves of axial symmetry. Limited-diffraction array beams [157–160] have been used for efficient computation of waves produced by a two-dimensional array transducer [159,160]. Angular spectrum decomposition has been used for the study [161], and various methods have been investigated [162].

4.3   APPLICATIONS OF LIMITED-DIFFRACTION BEAMS

4.3.1   Medical Ultrasound Imaging

Limited-diffraction beams are localized waves and are, in theory, propagation invariant. In practice, because the dimension of wave sources is always finite, these waves will eventually diffract. However, these waves have a large depth of field, meaning that they will propagate over a large distance without spreading. This property is useful in medical ultrasound imaging, where an extended depth of focus is needed to provide clear images over the entire depth of interest within the thickness of the human body. Studies on this subject have been reported in the literature (e.g., [15–17, 163–168]).

4.3.2   Tissue Characterization (Identification)

Due to the large depth of field of limited-diffraction beams, these beams may be used for tissue characterization (identification) [169–171]. For example, different tissues have different attenuations on ultrasound waves. If the waves diffract as they propagate, such as conventional focused waves, one has to compensate for the diffraction effects of the waves in the estimation of tissue attenuation. The compensation process could be computationally intensive and tedious. An example of tissue characterization with limited-diffraction beams is given in [171].

4.3.3   High-Frame-Rate Imaging

High-frame-rate two- and three-dimensional ultrasound imaging is important for visualizing fast-moving objects such as the heart. Based on our previous studies of ultrasound diffraction tomography [172–176] and limited-diffraction beams such as X-waves [41–53], we have developed the high-frame-rate imaging method [62–88]. Recently, the method has been extended to include steered plane wave and limited-diffraction array-beam transmissions [79–85].

4.3.4   Two-Way Dynamic Focusing

A two-way dynamic focusing method was developed by transmitting limited-diffraction array beams and receiving ultrasound echo signals with array beam weightings of the same parameters. This method increases the image field of view and image resolution due to enlarged coverage of spatial Fourier domain [177].

4.3.5   Medical Blood-Flow Measurements

Blood-flow velocity measurements and imaging are important for medical diagnoses [178–179]. However, with the conventional Doppler method, only flow velocity that is along the ultrasound beam can be measured. To measure the velocity vector, velocity components along and transverse to the beam are both needed. Limited-diffraction beams may help to measure the transverse component of the velocity more accurately, due to their spatial modulation properties [158,180,181].

4.3.6   Nondestructive Evaluation of Materials

Nondestructive evaluation (NDE) is important for many applications, such as finding defects in aircraft engines with ultrasound without slicing them apart or destroying them. Similar to medical imaging, limited-diffraction beams can also be applied to NDE on various industrial materials by getting images of a large depth of field [182,183].

4.3.7   Optical Coherent Tomography

Optical coherent tomography (OCT) uses the same principle of conventional ultrasound pulse-echo imaging. It is able to obtain microscopic images of a cross section along an optical beam. Similar to ultrasound imaging, limited-diffraction beams can be used to increase the depth of field of OCT [184].

4.3.8   Optical Communications

Limited-diffraction beams such as X-waves [41–43] are orthogonal in space. Because of this property, signals such as television programs in different channels can be sent over the same space from the same channel (carrier frequency). Limited-diffraction beams have been exploited to increase the capacity in communications using the property of their spatial orthogonality [185–186].

4.3.9   Reduction of Sidelobes in Medical Imaging

Limited-diffraction beams can maintain high resolution in medical imaging over a large depth of field. However, compared to focused beams at their focuses, limited-diffraction beams have higher sidelobes. Sidelobes may lower image contrast in ultrasound imaging, making the differentiation between benign and malignant tissues difficult. Various methods have been developed to reduce sidelobes of limited-diffraction beam in medical imaging [5,187–190].

4.4   CONCLUSIONS

Limited-diffraction beams are a class of waves that may be localized in both space and time and can propagate rigidly in free space or confined spaces to an infinite distance

in theory at superluminal speed. Because of the localized property and the fact that they are solutions to various wave equations, limited-diffraction beams may provide insight into various physical phenomena and may have theoretical significance. In addition, limited-diffraction beams can be produced approximately with a finite aperture and energy over a large depth of field, meaning that they can keep a small beam width over a large distance. This and other properties of limited-diffraction beams make them suitable for various applications, such as medical imaging, tissue characterization, blood-flow measurement, nondestructive evaluation of materials, and optical communications.

Acknowledgments

REFERENCES

1. J. A. Stratton, *Electromagnetic Theory,* McGraw-Hill, New York, 1941, p. 356.

2. J. Durnin, Exact solutions for nondiffracting beams: I. The scalar theory, *J. Opt. Soc. Am. A* **4**(4), 651–654 (1987).

3. J. Durnin, J. J. Miceli, Jr., and J. H. Eberly, Diffraction-free beams, *Phys. Rev. Lett.* **58**(15), 1499–1501 (Apr. 13, 1987).

4. J. Durnin, J. J. Miceli, Jr., and J. H. Eberly, *Experiments with Nondiffracting Needle Beams*, Optical Society of America, Washington, DC, 1987, p. 208; available from IEEE Service Center, Piscataway, NJ (cat. no. 87CH2391–1).

5. J.-y. Lu and J. F. Greenleaf, Sidelobe reduction for limited diffraction pulse-echo systems, *IEEE Trans. Ultrason. Ferroelectr. Freq. Control* **40**(6), 735–746 (Nov. 1993).

6. G. Indebetow, Nondiffracting optical fields: some remarks on their analysis and synthesis, *J. Opt. Soc. Am. A* **6**(1), 150–152 (Jan. 1989).

7. F. Gori, G. Guattari, and C. Padovani, Model expansion for J0-correlated Schell-model sources, *Opt. Commun.* **64**(4), 311–316 (Nov. 15, 1987).

8. K. Uehara and H. Kikuchi, Generation of near diffraction-free laser beams, *Appl. Phys. B* **48**, 125–129 (1989).

9. L. Vicari, Truncation of nondiffracting beams, *Opt. Commun.* **70**(4), 263–266 (Mar. 15, 1989).

10. M. Zahid and M. S. Zubairy, Directionally of partially coherent Bessel–Gauss beams, *Opt. Commun.* **70**(5), 361–364 (Apr. 1, 1989).

11. S. Y. Cai, A. Bhattacharjee, and T. C. Marshall, "Diffraction-free" optical beams in inverse free electron laser acceleration, *Nucl. Instrum. Methods Phys. Res. A* **272**(1–2), 481–484 (Oct. 1988).

12. J. Ojeda-Castaneda and A. Noyola-lglesias, Nondiffracting wavefields in grin and free-space, *Microwave Opt. Technol. Lett.* **3**(12), 430–433 (Dec. 1990).

13. D. K. Hsu, F. J. Margetan, and D. O. Thompson, Bessel beam ultrasonic transducer: fabrication method and experimental results, *Appl. Phys. Lett.* **55**(20), 2066–2068 (Nov. 13, 1989).

14. J. A. Campbell and S. Soloway, Generation of a nondiffracting beam with frequency independent beam width, *J. Acoust. Soc. Am.* **88**(5), 2467–2477 (Nov. 1990).

15. J.-y. Lu and J. F. Greenleaf, Ultrasonic nondiffracting transducer for medical imaging, *IEEE Trans. Ultrasonics, Ferroelectr. Freq. Control* **37**(5), 438–447, (Sept. 1990).

16. J.-y. Lu and J. F. Greenleaf, Pulse-echo imaging using a nondiffracting beam transducer, *Ultrasound Med. Biol.* **17**(3), 265–281 (May 1991).

17. J.-y. Lu and J. F. Greenleaf, Ultrasonic nondiffracting transducer, U.S. patent 5,081,995, Jan. 21, 1992.

18. J.-y. Lu and J. F. Greenleaf, A computational and experimental study of nondiffracting transducer for medical ultrasound, *Ultrason. Imag.* **12**(2), 146–147 (Apr. 1990).

19. J.-y. Lu and J. F. Greenleaf, Effect on nondiffracting beam of deleting central elements of annular array transducer, *Ultrason. Imag.* **13**(2), 203 (Apr. 1991).

20. J.-y. Lu and J. F. Greenleaf, Simulation of imaging contrast of nondiffracting beam transducer, *J. Ultrasound Med.* **10**(3) (suppl.), S4 (Mar. 1991).

21. J.-y. Lu, Theoretical study of medical ultrasonic nondiffracting transducers, presented at the Whitaker Foundation's 3rd Annual Conference, July 30–Aug. 1, 1993.

22. D. Ding and J.-y. Lu, Second harmonic generation of the nth-order Bessel beams, *Phys. Rev. E* **61**(2), 2038–2041 (Feb. 2000).

23. D. Ding and J.-y. Lu, Higher-order harmonics of limited diffraction Bessel beams, *J. Acoust. Soc. Am.* **107**(3), 1212–1214 (Mar. 2000).

24. P. Fox, J. Cheng, and J.-y. Lu, Fourier–Bessel field calculation and tuning of a CW annular array, *IEEE Trans. Ultrason. Ferroelectr. Freq. Control* **49**(9), 1179–1190 (Sept. 2002).

25. P. D. Fox, J. Cheng, and J.-y. Lu, Theory and experiment of Fourier–Bessel field calculation and tuning of a PW annular array, *J. Acoust. Soc. Am.* **113**(5), 2412–2423 (May 2003).

26. P. D. Fox, J. Cheng, and J.-y. Lu, Ultrasound pulse modeling and tuning with Fourier–Bessel method for an annular array, *Ultrason. Imag.* **22**(4), 257 (Oct. 2000).

27. P. Fox and J.-y. Lu, Modelling of pulsed annular arrays using limited diffraction Bessel beams, *Ultrasound Med.* **20**(3) (suppl.), S66 (Mar. 2001).

28. P. Fox, J.-y. Lu, S. Holm, and F. Tranquart, Connection between X-waves, Fourier–Bessel series and optimal modeling aperture for circular symmetric arrays, *2005 IEEE Ultrasonics Symposium Proceedings*, 05CH37716C, Vol. 2, 2005, pp. 1644–1647.

29. J.-y. Lu, Construction of limited diffraction beams with Bessel bases, *1995 IEEE Ultrasonics Symposium Proceedings*, 95CH35844, Vol. 2, 1995, pp. 1393–1397.

30. J.-y. Lu, Designing limited diffraction beams, *IEEE Trans. Ultrason. Ferroelectr. Freq. Control* **44**(1), 181–193 (Jan. 1997).

31. J. N. Brittingham, Focus wave modes in homogeneous Maxwell's equations: transverse electric mode, *J. Appl. Phys.* **54**(3), 1179–1189 (1983).

32. R. W. Ziolkowski, Exact solutions of the wave equation with complex source locations, *J. Math. Phys.* **26**(4), 861–863 (Apr. 1985).

33. R. W. Ziolkowski, D. K. Lewis, and B. D. Cook, Evidence of localized wave transmission, *Phys. Rev. Lett.* **62**(2), 147–150 (Jan. 9, 1989).

34. A. M. Shaarawi, I. M. Besieris, and R. W. Ziolkowski, Localized energy pulse train launched from an open, semi-infinite, circular waveguide, *J. Appl. Phys.* **65**(2), 805–813 (1989).

35. I. M. Besieris, A. M. Shaarawi, and R. W. Ziolkowski, A bidirectional traveling plane wave representation of exact solutions of the scalar wave equation, *J. Math. Phys.* **30**(6), 1254–1269 (1989).

36. E. Heyman, B. Z. Steinberg, and L. B. Felsen, Spectral analysis of focus wave modes, *J. Opt. Soc. Am. A* **4**(11), 2081–2091 (Nov. 1987).

37. R. W. Ziolkowski, Localized transmission of electromagnetic energy, *Phys. Rev. A* **39**(4), 2005–2033 (Feb. 15, 1989).

38. J. V. Candy, R. W. Ziolkowski, and D. K. Lewis, Transient waves: reconstruction and processing, *J. Acoust. Soc. Am.* **88**(5), 2248–2258 (Nov. 1990).

39. J. V. Candy, R. W. Ziolkowski, and D. K. Lewis, Transient wave estimation: a multichannel deconvolution application, *J. Acoust. Soc. Am.* **88**(5), 2235–2247 (Nov. 1990).

40. R. W. Ziolkowski and D. K. Lewis, Verification of the localized wave transmission effect, *J. Appl. Phys.* **68**(12), 6083–6086, (Dec. 15, 1990).

41. J.-y. Lu and J. F. Greenleaf, Theory and acoustic experiments of nondiffracting X-waves, *1991 IEEE Ultrasonics Symposium Proceedings*, 91CH3079-1, Vol. 2, 1991, pp. 1155–1159.

42. J.-y. Lu and J. F. Greenleaf, Nondiffracting X-waves: exact solutions to free-space scalar wave equation and their finite aperture realizations, *IEEE Trans. Ultrason. Ferroelectr. Freq. Control* **39**(1), 19–31(Jan. 1992).

43. J.-y. Lu and J. F. Greenleaf, Experimental verification of nondiffracting X-waves, *IEEE Trans. Ultrason. Ferroelectr. Freq. Control* **39**(3), 441–446 (May 1992).

44. J.-y. Lu, H. Zou, and J. F. Greenleaf, A new approach to obtain limited diffraction beams, *IEEE Trans. Ultrason. Ferroelectr. Freq. Control* **42**(5), 850–853 (Sept. 1995).

45. H. Zou, J.-y. Lu, and J. F. Greenleaf, Obtaining limited diffraction beams with the wavelet transform, *1993 IEEE Ultrasonics Symposium Proceedings*, 93CH3301-9, Vol. 2, 1993, pp. 1087–1090.

46. J.-y. Lu and A. Liu, An X-wave transform, *IEEE Trans. Ultrason. Ferroelectr. Freq. Control* **47**(6), 1472–1481 (Nov. 2000).

47. J.-y. Lu and A. Liu, Representation of solutions to wave equation with X-waves, *Ultrason. Imag.* **21**(1), 70 (Jan. 1999).

48. W. A. Rodrigues, Jr., and J.-y. Lu, On the existence of undistorted progressive waves (UPWs) of arbitrary speeds $0 < v < \infty$ in nature, *Found. Phys.* **27**(3), 435–508 (Mar. 1997).

49. Tai K. Song, J.-y. Lu, and J. F. Greenleaf, Modified X-waves with improved field properties, *Ultrason. Imag.* **15**(1), 36–47 (Jan. 1993).

50. J.-y. Lu, and J. F. Greenleaf, Formation and propagation of limited diffraction beams, in Yu Wei and Ben-li Gu, Eds; *Acoustical Imaging*, Vol. 20, Kluwer Academic/Plenum, NY, 1993, pp. 331–343.

51. J.-y. Lu and J. F. Greenleaf, Comparison of sidelobes of limited diffraction beams and localized waves, in J. P. Jones, Ed., *Acoustical Imaging*, Vol. 21, Kluwer Academic/Plenum, NY, 1995, pp. 145–152.

52. J.-y. Lu and J. F. Greenleaf, Steering of limited diffraction beams with a two-dimensional array transducer, *1992 IEEE Ultrasonics Symposium Proceedings*, 92CH3118-7, Vol. 1, 1992, pp. 603–607.

53. J.-y. Lu and J. F. Greenleaf, A study of two-dimensional array transducers for limited diffraction beams, *IEEE Trans. Ultrason. Ferroelectr. Frequency Control* **41**(5), 724–739 (Sep. 1994).

54. J.-y. Lu, J. F. Greenleaf, and E. Recami, Limited diffraction solutions to Maxwell and Schrödinger equations, LANL archives physics/9610012, Report INFN/FM-96/01, Instituto Nagionole de Fisica Nucleare, Frascati, Italy, Oct. 1996.

55. C. Day, Intense X-shaped pulses of light propagate without spreading in water and other dispersive media, "Search and Discovery" column of *Phys. Today* **57**(10), 25–26 (Oct. 2004).

56. P. Saari and K. Reivelt, Evidence of X-shaped propagation-invariant localized light waves, *Phys. Rev. Lett.* **79**, 4135–4138 (1997).

57. I. Besieris, M. Abdel-Rahman, A. Shaarawi, and A. Chatzipetros, Two fundamental representations of localized pulse solutions to the scalar wave equation, *Prog. Electromagn. Res.* **19**, 1–48 (1998).

58. P. Saari and K. Reivelt, Generation and classification of localized waves by Lorentz transformations in Fourier space, *Phys. Rev. E* **69**, 036612 (2004).

59. M. Zamboni-Rached, K. Z. Nóbrega, E. Recami, and H. E. Hernández-Figueroa, Superluminal X-shaped beams propagating without distortion along a coaxial guide, *Phys. Rev. E* **66**, 046617 (2002).

60. M. Zamboni-Rached, E. Recami, and F. Fontana, Superluminal localized solutions to Maxwell equations propagating along a normal-sized waveguide, *Phys. Rev. E* **64**, 066603 (2001).

61. J. Salo, A. T. Friberg, and M. M. Salomaa, Orthogonal X-waves, *J. Phys. A Math. Gen.* **34**, 9319–9327 (2001).

62. J.-y. Lu, 2D and 3D high frame rate imaging with limited diffraction beams, *IEEE Trans. Ultrason. Ferroelectr. Freq. Control* **44**(4), 839–856 (July 1997).

63. J.-y. Lu, Experimental study of high frame rate imaging with limited diffraction beams, *IEEE Trans. Ultrason. Ferroelectr. Freq. Control* **45**(1), 84–97 (Jan. 1998).

64. J.-y. Lu, Limited diffraction beams for high frame rate 2D and 3D pulse-echo imaging, *J. Ultrasound Med.* **16**(3) (suppl.), S10 (Mar. 1997).

65. J.-y. Lu and J. F. Greenleaf, High frame rate imaging with limited diffraction beams, U. S. patent 5,720,708, Feb. 24, 1998.

66. H. Peng and J.-y. Lu, High frame rate 2D and 3D imaging with a curved or cylindrical array, *2002 IEEE Ultrasonics Symposium Proceedings*, 02CH37388, Vol. 2, 2002, pp. 1725–1728.

67. H. Peng and J.-y. Lu, Construction of high frame rate images with Fourier transform, *J. Acoust. Soc. Am.* **111**(5), pt. 2, 2385–2386 (2002).

68. J.-y. Lu and A. Liu, Comparison of high-frame rate and delay-and-sum imaging methods, *J. Acoust. Soc. Am.* **106**(4), pt. 2, 2136 (Oct. 1999).

69. J.-y. Lu and S. He, High frame rate imaging with a small number of array elements, *IEEE Trans. Ultrason. Ferroelectr. Freq. Control* **46**(6), 1416–1421 (Nov. 1999).

70. J.-y. Lu and S. He, Reducing number of elements of transducer arrays in Fourier image construction method, *1998 IEEE Ultrasonics Symposium Proceedings*, 98CH36102, Vol. 2, 1998, pp. 1619–1622.

71. J.-y. Lu and S. He, Effects of phase aberration on high frame rate imaging, *Ultrasound Med. Bio.* **26**(1), 143–152 (2000).

72. J.-y. Lu, Assessment of phase aberration effects on high frame rate imaging, *Ultrason. Imag.* **19**(1), 53 (Jan. 1997).

73. J.-y. Lu, A study of signal-to-noise ratio of the Fourier method for construction of high frame rate images, in Hua Lee, Ed., *Acoustical Imaging*, vol. **24**, Kluwer Academic/Plenum, NY, 2000, pp. 401–405.

74. J.-y. Lu, J. Cheng, and J. Wang, High frame rate imaging system for limited diffraction array beam imaging with square-wave aperture weightings, *IEEE Trans. Ultrason. Ferroelectr. Freq. Control* **53**(10), 1796–1812 (October 2006).

75. J.-y. Lu and J. L. Waugaman, Development of a linear power amplifier for high frame rate imaging system, *2004 IEEE Ultrasonics Symposium Proceedings*, 04CH37553C, Vol. 2, 2004, pp. 1413–1416.

76. J.-y. Lu, A multimedia example, *IEEE Trans. Ultrason. Ferroelectr. Freq. Control* **50**(9), 1078 (Sep. 2003).

77. A. Liu, J. Wang, and J.-y. Lu, Logic design and implementation of FPGA for a high frame rate ultrasound imaging system, *J. Acoust. Soc. Am.* **111**(5), pt. 2, 2484 (2002).

78. J. Wang, J. L. Waugaman, A. Liu, and J.-y. Lu, Design and construction of a high frame rate imaging system, *Acoust. Soc. Am.* **111**(5), pt. 2, 2484 (2002).

79. J. Cheng and J.-y. Lu, Extended high frame rate imaging method with limited diffraction beams, *IEEE Trans. Ultrason. Ferroelectr. Freq. Control* **53**(5), 880–899 (May 2006).

80. J. Cheng and J.-y. Lu, Fourier based imaging method with steered plane waves and limited-diffraction array beams, *2005 IEEE Ultrasonics Symposium Proceedings*, 05CH37716C, Vol. 2, 2005, pp. 1976–1979.

81. J. Wang and J.-y. Lu, A study of motion artifacts of Fourier-based image construction, *2005 IEEE Ultrasonics Symposium Proceedings*, 05CH37716C, Vol. 2, 2005, pp. 1439–1442.

82. J. Wang and J.-y. Lu, Motion artifacts of extended high frame rate imaging, *IEEE Trans. Ultrason. Ferroelectr. Freq. Control* **54**(7), 1303–1315 (July 2007).

83. J.-y. Lu and J. Wang, Square-wave aperture weightings for reception beam forming in high frame rate imaging, *2006 IEEE Ultrasonics Symposium Proceedings* 06CH37777, Vol. 1, 2006, pp. 124–127.

84. J.-y. Lu, Z. Wang, and S. Kwon, Blood flow velocity vector imaging with high frame rate imaging methods, *2006 IEEE Ultrasonics Symposium Proceedings* 06CH37777, Vol. 2, 2006, pp. 963–966.

85. J. Wang and J.-y. Lu, Effects of phase aberration and noise on extended high frame rate imaging, *Ultrasonic Imaging* **29**(2), 105–121 (April 2007).

86. J.-y. Lu and S. He, Increasing field of view of high frame rate ultrasonic imaging, *J. Acoust. Soc. Am.* **107**(5), pt. 2, 2779 (May 2000).

87. J.-y. Lu, Nonlinear processing for high frame rate imaging, *J. Ultrasound Med.* 18(3), (suppl.), S50 (Mar. 1999).

88. G. Wade, Human uses of ultrasound: ancient and modern, *Ultrasonics*, **38**, 1–5 (2000).

89. M. A. Porras, A. Parola, D. Faccio, A. Dubietis, and P. Di Trapani, Nonlinear unbalanced Bessel beams: stationary conical waves supported by nonlinear losses, *Phys. Rev. Lett.* **93**, 153902 (2004).

90. M. Kolesik, E. M. Wright, and J. V. Moloney, Dynamic nonlinear X-waves for femtosecond pulse propagation in water, *Phys. Rev. Lett.* **92**, 253901 (2004).

91. C. Conti and S. Trillo, Nonspreading wave packets in three dimensions formed by an ultracold Bose gas in an optical lattice, *Phys. Rev. Lett.* **92**, 120404 (2004).

92. P. Di Trapani, G. Valiulis, A. Piskarskas, O. Jedrkiewicz, J. Trull, C. Conti, and S. Trillo, Spontaneously generated X-shaped light bullets, *Phys. Rev. Lett.* **91**, 093904 (2003).

93. C. Conti, S. Trillo, P. Di Trapani, G. Valiulis, A. Piskarskas, O. Jedrkiewicz, and J. Trull, Nonlinear electromagnetic X-waves, *Phys. Rev. Lett.* **90**, 170406 (2003).

94. J. Salo, J. Fagerholm, A. T. Friberg, and M. M. Salomaa, Nondiffracting bulk-acoustic X-waves in crystals, *Phys. Rev. Lett.* **83**, 1171–1174 (1999).

95. T. Wulle and S. Herminghaus, Nonlinear optics of Bessel beams, *Phys. Rev. Lett.* **70**, 1401–1404 (1993).

96. S. Longhi and D. Janner, X-shaped waves in photonic crystals, *Phys. Rev. B* **70**, 235123 (2004).

97. S. Longhi, Localized and nonspreading spatiotemporal Wannier wave packets in photonic crystals, *Phys. Rev. E* **71**, 016603 (2005).

98. A. Ciattoni and P. Di Porto, Electromagnetic nondiffracting pulses in lossless isotropic plasmalike media, *Phys. Rev. E* **70**, 035601(R) (2004).

99. M. A. Porras, and P. Di Trapani, Localized and stationary light wave modes in dispersive media, *Phys. Rev. E* **69**, 066606 (2004).

100. A. Ciattoni and P. Di Porto, One-dimensional nondiffracting pulses, *Phys. Rev. E* **69**, 056611 (2004).

101. A. Ciattoni, C. Conti, and P. Di Porto, Vector electromagnetic X waves, *Phys. Rev. E* **69**, 036608 (2004).

102. E. Recami, M. Zamboni-Rached, and C. A. Dartora, Localized X-shaped field generated by a superluminal electric charge, *Phys. Rev. E* **69**, 027602 (2004).

103. J. Trull, O. Jedrkiewicz, P. Di Trapani, A. Matijosius, A. Varanavicius, G. Valiulis, R. Danielius, E. Kucinskas, A. Piskarskas, and S. Trillo, Spatiotemporal three-dimensional mapping of nonlinear X waves, *Phys. Rev. E* **69**, 026607 (2004).

104. S. Longhi, Parametric amplification of spatiotemporal localized envelope waves, *Phys. Rev. E* **69**, 016606 (2004).

105. S. Longhi, Spatial-temporal Gauss–Laguerre waves in dispersive media, *Phys. Rev. E* **68**, 066612 (2003).

106. R. W. Ziolkowski and Ching-Ying Cheng, Existence and design of trans-vacuum-speed metamaterials, *Phys. Rev. E* **68**, 026612 (2003).

107. O. Jedrkiewicz, J. Trull, G. Valiulis, A. Piskarskas, C. Conti, S. Trillo, and P. Di Trapani, Nonlinear X waves in second-harmonic generation: experimental results, *Phys. Rev. E* **68**, 026610 (2003).

108. M. A. Porras, G. Valiulis, and P. Di Trapani, Unified description of Bessel X waves with cone dispersion and tilted pulses, *Phys. Rev. E* **68**, 016613 (2003).

109. C. Conti, X wave-mediated instability of plane waves in Kerr media, *Phys. Rev. E* **68**, 016606 (2003).

110. M. A. Porras, I. Gonzalo, and A. Mondello, Pulsed light beams in vacuum with superluminal and negative group velocities, *Phys. Rev. E* **67**, 066604 (2003).

111. J. Salo and M. M. Salomaa, Nondiffracting waves in anisotropic media, *Phys. Rev. E* **67**, 056609 (2003).

112. M. Zamboni-Rached, F. Fontana, and E. Recami, Superluminal localized solutions to Maxwell equations propagating along a waveguide: the finite-energy case, *Phys. Rev. E* **67**, 036620 (2003).

113. K. Reivelt and P. Saari, Experimental demonstration of realizability of optical focus wave modes, *Phys. Rev. E* **66**, 056611 (2002).

114. A. M. Shaarawi, B. H. Tawfik, and I. M. Besieris, Superluminal advanced transmission of X waves undergoing frustrated total internal reflection: the evanescent fields and the Goos–Hänchen effect, *Phys. Rev. E* **66**, 046626 (2002).

115. K. Reivelt and P. Saari, Optically realizable localized wave solutions of the homogeneous scalar wave equation, *Phys. Rev. E* **65**, 046622 (2002).

116. M. A. Porras, Diffraction effects in few-cycle optical pulses, *Phys. Rev. E* **65**, 026606 (2002).

117. R. W. Ziolkowski, Superluminal transmission of information through an electromagnetic metamaterial, *Phys. Rev. E* **63**, 046604 (2001).

118. Z. L. Horváth and Z. Bor, Diffraction of short pulses with boundary diffraction wave theory, *Phys. Rev. E* **63**, 026601 (2001).

119. M. A. Porras, R. Borghi, and M. Santarsiero, Few-optical-cycle Bessel–Gauss pulsed beams in free space, *Phys. Rev. E* **62**, 5729–5737 (2000).

120. J. Salo, J. Fagerholm, A. T. Friberg, and M. M. Salomaa, Unified description of nondiffracting X and Y waves, *Phys. Rev. E* **62**, 4261–4275 (2000).

121. A. Ranfagni and D. Mugnai, Possibility of superluminal behaviors for X-like and Zenneck waves, *Phys. Rev. E* **58**, 6742–6745 (1998).

122. J. Fagerholm, A. T. Friberg, J. Huttunen, D. P. Morgan, and M. M. Salomaa, Angular-spectrum representation of nondiffracting X waves, *Phys. Rev. E* **54**, 4347–4352 (1996).

123. D. Power and R. Donnelly, Spherical scattering of superpositions of localized waves, *Phys. Rev. E* **48**, 1410–1417 (1993).

124. J.-y. Lu, H. Zou, and J. F. Greenleaf, Biomedical ultrasound beam forming, *Ultrasound Med. Bio.* **20**(5), 403–428 (July 1994).

125. J.-y. Lu and J. F. Greenleaf, Diffraction-limited beams and their applications for ultrasonic imaging and tissue characterization, in F. L. Lizzi, Ed., *New Developments in Ultrasonic Transducers and Transducer Systems*, *Proc. SPIE* **1733**, 92–119 (1992).

126. J.-y. Lu, Principle and applications of limited diffraction beams, *Acta Phys. Sin.* **8** (suppl.) 22–26, (Aug. 1999).

127. J.-y. Lu, Principle and applications of limited diffraction beams, *Proceedings of the 7th International Workshop on Modern Acoustics—Ultrasonics*, 1998, p. 8.

128. J.-y. Lu, New development in beam propagation, *J. Ultrasound Med.* **12**(3) (suppl.), S29 (Mar. 1993).

129. J.-y. Lu, Engineering applications of limited diffraction beams, *J. Acoust. Soc. Am.* **117**(4), pt. 2, 2446 (2005).

130. J.-y. Lu, Limited diffraction beams and their applications on signal processing, *J. Acoust. Soc. Am.* **106**(4), pt. 2, 2125 (Oct. 1999).

131. J.-y. Lu, Limited diffraction beams: their principles and potential applications, presented at the Ultrasonic Transducer Engineering Workshop, Aug. 16–18, (1995).

132. J.-y. Lu, T. Kinter, and J. F. Greenleaf, Measurement and dynamic display of acoustic wave pulses, *1989 IEEE Ultrasonics Symposium Proceedings*, 89CH2791-2, Vol. 1, 1989, pp. 673–676.

133. J.-y. Lu, R. R. Kinnick, J. F. Greenleaf, and C. M. Sehgal, Multi-electrical excitations of a transducer for ultrasonic imaging, in H. Lee and G. Wade, Eds., *Acoustical Imaging*, Vol. 18, Kluwer Academic/Plenum, NY, 1990, pp. 511–519.

134. J.-y. Lu and J. F. Greenleaf, Evaluation of transducers with near-field scanning of their surfaces, *1994 IEEE Ultrasonics Symposium Proceedings*, 94CH3468-6, Vol. 2, 1994, pp. 1163–1167.

135. T. A. Pitts, J. F. Greenleaf, J.-y. Lu, and R. R. Kinnick, Tomographic Schlieren imaging for measurement of beam pressure and intensity, *1994 IEEE Ultrasonics Symposium Proceedings*, 94CH3468-6, Vol. 3, 1994, pp. 1665–1668.

136. W. H. Press, B. P. Flannery, S. A. Teukolsky, and W. T. Vetterling, *Numerical Recipes in C*, Cambridge University Press, Cambridge, 1989, Chaps. 2 and 14.

137. M. Zamboni-Rached, Stationary optical wave fields with arbitrary longitudinal shape by superposing equal frequency Bessel beams: frozen waves, *Opt. Express* **12**(17), 4001–4006 (Aug. 23, 2004).

138. M. Zamboni-Rached, E. Recami, and H. E. Hernández-Figueroa, Theory of frozen waves: modeling the shape of stationary wave fields, *J. Opt. Soc. Am. A* **22**(11), 2465–2475 (Nov. 2005).

139. V. Garcés-Chávez, D. McGloin, H. Melville, W. Sibbett, and K. Dholakia, Simultaneous micromanipulation in multiple planes using a self-reconstructing light beam, *Nature* **419**, 145–147 (Sept 12, 2002).

140. J. A. Campbell and S. Soloway, Generation of a nondiffracting beam with frequency independent beam width, *J. Acoust. Soc. Am.* **88**(5), 2467–2477 (Nov. 1990).

141. M. S. Patterson and F. S. Foster, Acoustic fields of conical radiators, *IEEE Trans. Son. Ultrason.* **SU-29**(2), 83–92 (Mar. 1982).

142. J. H. Mcleod, The axicon: a new type of optical element, *J. Opt. Soc. Am.* **44**, 592 (1954).

143. Fayyazuddin and Riazuddin, *Quantum Mechanics*, World Scientific, Singapore, 1990, Chap. 18.

144. T. R. Sandin, *Essentials of Modern Physics*, Addison-Wesley, Reading, MA, 1989, p. 146.

145. J. R. Meyer-Arendt, *Introduction to Classical and Modern Optics*, Prentice-Hall, Englewood Cliffs, NJ, 1972, Chap. 6 .

146. R. W. Ziolkowski, Localized transmission of electromagnetic energy, *Phys. Rev. A* **39** 2005–2033 (1989).

147. J.-y. Lu, Frequency quantized nondiffracting X waves in a confined space, prepared on July 25, 1991 and revised on March 7, 1992 for the *Journal of Acoustical Society of America*. However, it is unpublished but was acknowledged on page 5 in M. Zamboni-Rached, E. Recami, and F. Fontana, Superluminal localized solutions to Maxwell equations propagating along a normal-sized waveguide, *Phys. Rev. E* **64**, 066603 (2001).

148. A. M. Shaarawi, I. M. Besieris, and R. W. Ziolkowski, Localized energy pulse trains launched from an open, semi-infinite, circular wave guide, *J. Appl. Phys.* **65**(2), 805–813 (Jan. 15, 1989).

149. R. W. Ziolkowski, I. M. Besieris, and A. M. Shaarawi, Localized wave representations of acoustic and electromagnetic radiation, *Proc. IEEE* **79**(10), 1371–1377, (Oct. 1991).

150. J. R. Meyer-Arendt, *Introduction to Classical and Modern Optics*, Prentice-Hall, Englewood Cliffs, NJ, 1972, Chap. 6.

151. R. Bracewell, *The Fourier Transform and Its Applications*, McGraw-Hill, New York, 1965, Chaps. 4 and 6.

152. J.-y. Lu, Bowtie limited diffraction beams for low-sidelobe and large depth of field imaging, *IEEE Trans. Ultrason. Ferroelectr. Freq. Control* **42**(6), 1050–1063 (Nov. 1995).

153. J.-y. Lu, Producing bowtie limited diffraction beams with synthetic array experiment, *IEEE Trans. Ultrason. Ferroelectr. Freq. Control* **43**(5), 893–900 (Sept. 1996).

154. J.-y. Lu, Method for reducing sidelobes of limited diffraction pulse-echo images, U.S. patent 5,492,121, Feb. 20, 1996.

155. J.-y. Lu and J. F. Greenleaf, Unsymmetrical limited diffraction beams for sidelobe reduction, *Ultrasound Med.* **14**(3) (supp.), S36 (Mar. 1995).

156. J.-y. Lu, Experiment with bowtie limited diffraction beams, *Ultrason. Imag.* **18**(1), 41 (Jan. 1996).

157. J.-y. Lu, Limited diffraction array beams, *Int. J. Imag. Sys. Technol.* **8**(1), 126–136 (Jan. 1997).

158. J.-y. Lu, Improving accuracy of transverse velocity measurement with a new limited diffraction beam, *1996 IEEE Ultrasonics Symposium Proceedings*, 96CH35993, Vol. 2, 1996, pp. 1255–1260.

159. J.-y. Lu and J. Cheng, Field computation for two-dimensional array transducers with limited diffraction array beams, *Ultrason. Imag.* **27**(4), 237–255 (Oct. 2005).

160. J.-y. Lu and J. Cheng, Efficient computation of field of 2D array with limited diffraction array beams, *J. Acoust. Soc. Am.* **109**(5), pt. 2, 2397–2398 (2001).

161. J. Cheng and J.-y. Lu, A study of angular spectrum and limited diffraction beams for calculation of field of array transducers, *J. Acoust. Soc. Am.* **111**(5), pt. 2, 2483 (2002).

162. H. Peng, Z. Zhang, and J.-y. Lu, A study of simulation methods of limited diffraction beams, *J. Acoust. Soc. Am.* **108**(5), pt. 2, 2595 (Nov. 2000).

163. J.-y. Lu, Tai K. Song, R. R. Kinnick, and J. F. Greenleaf, In vitro and in vivo real-time imaging with ultrasonic limited diffraction beams, *IEEE Trans. Med. Imag.* **12**(4), 819–829 (Dec. 1993).

164. J.-y. Lu, T.-K. Song, R. R. Kinnick, and J. F. Greenleaf, Real-time imaging with limited diffraction beams, *Ultrason. Imag.* **15**(2), 176 (Apr. 1993).

165. J.-y. Lu, T.-K. Song, R. R. Kinnick, J. F. Greenleaf, J. E. Meredith, and J. W. Charboneau, A general-purpose real-time scanner for evaluation of beam geometry in medical imaging, *J. Ultrasound Med.* **13**(3) (suppl.), S40 (Mar. 1994).

166. J.-y. Lu, M. Fatemi, and J. F. Greenleaf, Pulse-echo imaging with X wave, in P. Tortoli and L. Masotti, Eds., *Acoustical Imaging*, Vol. 22, Kluwer Academic/Plenum, NY, 1996, pp. 191–196.

167. J.-y. Lu and J. F. Greenleaf, Experiment of imaging contrast of Bessel nondiffracting beam transducer, *J. Ultrasound Med.* **11**(3) (suppl.), S43 (Mar. 1992).

168. J.-y. Lu, J. Wang, H. Peng, and J. Cheng, Increasing frame rate of limited diffraction imaging system with code excitations, in R. G. Maev, Ed., *Acoustical Imaging*, Vol. 26, Kluwer Academic/Plenum, NY, 2002, pp. 467–475.

169. K. F. Dajani, S. Salles-Cunha, H. G. Beebe, and J.-y. Lu, Ultrasonographic volumetry of atherosclerotic plaques, *J. Vasc. Technol.* **26**(2), 89–97 (June 2002).

170. K. F. Dajani, R. K. Vincent, S. Salles-Cunha, J.-y. Lu, and H. G. Beebe, Multi-frequency ultrasound imaging for carotid plaque characterization: a feasibility study, *Ultrason. Imag.* **21**(4), 292–293 (Oct. 1999).

171. J.-y. Lu and J. F. Greenleaf, Evaluation of a nondiffracting transducer for tissue characterization, *1990 IEEE Ultrasonics Symposium Proceedings*, 90CH2938-9, Vol. 2, 1990, pp. 795–798.

172. J.-y. Lu, A computational study for synthetic aperture diffraction tomography: interpolation versus interpolation-free, in L. W. Kessler, Ed., *Acoustical Imaging*, Vol. 16, Kluwer Academic/Plenum, NY, 1988, pp. 421–443.

173. J.-y. Lu and Y. Wei, An improvement of the Fourier-domain interpolation reconstruction algorithms for synthetic aperture diffraction tomography, *Appl. Acoust.* (Chinese quarterly) **8**(1), 1–5 (1989).

174. J.-y. Lu and Y. Wei, A study of the Fourier-domain interpolation reconstruction algorithms for synthetic aperture diffraction tomography, *Chin. J. Med. Imag. Technol.* **4**(1), 47 (1988).

175. J.-y. Lu and Y. Wei, A new method for quantitative reflection imaging, in Hiroshi Shimizu, Noriyoshi Chubachi, and Jun-ichi Kushibiki, Eds., *Acoustical Imaging*, Vol. 17, 1989, pp. 533–541.

176. J.-y. Lu and Y. Wei, Experiments for a new quantitative reflection imaging method, *Phys. Med. Bio.* **33** (suppl. 1), 291 (1988).

177. J.-y. Lu, Transmit–receive dynamic focusing with limited diffraction beams, *1997 IEEE Ultrasonics Symposium Proceedings*, 97CH36118, Vol. 2, 1997, pp. 1543–1546.

178. S. He, K. F. Dajani, and J.-y. Lu, Doppler beam steering for blood flow velocity vector imaging, in M. Halliwell and P. N. T. Wells, Eds., *Acoustical Imaging*, Vol. 25, Kluwer Academic/Plenum, NY, 2000, pp. 443–448.

179. J.-y. Lu, S. He, and K. F. Dajani, Ultrasound storage correlator arrays for real-time blood flow velocity vector imaging, in M. Halliwell and P. N. T. Wells, Eds., *Acoustical Imaging*, Vol. 25, 2000, pp. 427–436.

180. J.-y. Lu, X.-L. Xu, H. Zou, and J. F. Greenleaf, Application of Bessel beam for Doppler velocity estimation, *IEEE Trans. Ultrason. Ferroelectr. Freq. Control* **42**(4), 649–662 (July 1995).

181. J.-y. Lu, X.-L. Xu, H. Zou, and J. F. Greenleaf, Modeling and experiment of Doppler shift and its spectral broadening for a Bessel beam, *Ultrason. Imag.* **16**(1), 53–54 (Jan. 1994).

182. J.-y. Lu and J. F. Greenleaf, Producing deep depth of field and depth-independent resolution in NDE with limited diffraction beams, *Ultrason. Imag.* **15**(2), 134–149 (Apr. 1993).

183. J.-y. Lu and J. F. Greenleaf, Nondestructive evaluation of materials with a Bessel transducer, *Ultrason. Imag.* **14**(2), 203–204 (Apr. 1992).

184. J.-y. Lu, J. Cheng, and B. Cameron, Low sidelobe limited diffraction optical coherence tomography, *Proc. SPIE* **4619**, 300–311 (2002).

185. J.-y. Lu and S. He, Optical X waves communications, *Opt. Commun.* **161**, 187–192 (Mar. 15, 1999).

186. J.-y. Lu, High-speed transmissions of images with limited diffraction beams, in S. Lees and L. A. Ferrari, Eds., *Acoustical Imaging*, Vol. 23, Kluwer Academic/Plenum, NY, 1997, pp. 249–254.

128   ULTRASONIC IMAGING WITH LIMITED-DIFFRACTION BEAMS

187. J.-y. Lu and J. F. Greenleaf, A study of sidelobe reduction for limited diffraction beams, *1993 IEEE Ultrasonics Symposium Proceedings*, 93CH3301-9, Vol. 2, 1993, pp. 1077–1082.

188. S. He and J.-y. Lu, Sidelobe reduction of limited diffraction beams with Chebyshev aperture apodization, *J. Acoust. Soc. Am*. **107**(6), 3556–3559 (June 2000).

189. J.-y. Lu, J. Cheng, and H. Peng, Sidelobe reduction of images with coded limited diffraction beams, *2001 IEEE Ultrasonics Symposium Proceedings*, 01CH37263, Vol. 2, 2001, pp. 1565–1568.

190. J.-y. Lu and J. F. Greenleaf, Sidelobe reduction of nondiffracting pulse-echo images by deconvolution, *Ultrason. Imag.* **14**(2), 203 (Apr. 1992).